NASA Contractor Report 189638
ICASE Report No. 92–16

ICASE

ON TESTING MODELS FOR THE PRESSURE-STRAIN CORRELATION OF TURBULENCE USING DIRECT SIMULATIONS

C. G. Speziale
T. B. Gatski
S. Sarkar

Contract No. NAS1–18605
April 1992

Institute for Computer Applications in Science and Engineering
NASA Langley Research Center
Hampton, Virginia 23665–5225

Operated by the Universities Space Research Association

National Aeronautics and
Space Administration

Langley Research Center
Hampton, Virginia 23665-5225

ON TESTING MODELS FOR THE PRESSURE-STRAIN CORRELATION OF TURBULENCE USING DIRECT SIMULATIONS

Charles G. Speziale*
ICASE, NASA Langley Research Center
Hampton, VA 23665

Thomas B. Gatski
NASA Langley Research Center
Hampton, VA 23665

Sutanu Sarkar*
ICASE, NASA Langley Research Center
Hampton, VA 23665

ABSTRACT

Direct simulations of homogeneous turbulence have, in recent years, come into widespread use for the evaluation of models for the pressure-strain correlation of turbulence. While work in this area has been beneficial, the increasingly common practice of testing the slow and rapid parts of these models separately in uniformly strained turbulent flows is shown in this paper to be unsound. For such flows, the decomposition of models for the pressure-strain correlation into slow and rapid parts is ambiguous. Consequently, when tested in this manner, misleading conclusions can be drawn about the performance of pressure-strain models. This point is amplified by illustrative calculations of homogeneous shear flow where other pitfalls in the evaluation of models are also uncovered. More meaningful measures for testing the performance of pressure-strain models in uniformly strained turbulent flows are proposed and the implications for turbulence modeling are discussed.

*Research was supported by the National Aeronautics and Space Administration under NASA Contract No. NAS1-18605 while the first and third authors were in residence at the Institute for Computer Applications in Science and Engineering (ICASE), NASA Langley Research Center, Hampton, VA 23665.

1. INTRODUCTION

Direct numerical simulations (DNS) of turbulent flows have provided a powerful new tool for the testing and screening of turbulence models. Turbulence quantities that are not directly measurable can now be computed accurately – for a variety of benchmark turbulent flows – in far more detail than that which can be extrapolated from physical experiments. The pressure-strain correlation, which plays a pivotal role in the formulation of Reynolds stress transport models, represents a prime example where DNS data bases have provided a wealth of interesting new information.[1] During the past decade – beginning perhaps, with the work of Rogallo[2] – models for the pressure-strain correlation have been tested using DNS data bases for homogeneous turbulent flows. In the most recent such work, it has become a common practice to decompose models for the pressure strain correlation into slow and rapid parts and to compare the model predictions for these parts separately with DNS data bases.[3–5] This approach seemed attractive since it would provide a gauge on the performance of each part of a model for the pressure-strain correlation. Prior to the advent of direct simulations of turbulence, such comparisons were not possible since the slow and rapid parts of the pressure-strain correlation cannot be measured, even by indirect means. However, in uniformly strained turbulent flows, this procedure can lead to misleading results. The main purpose of the present paper is demonstrate this point along with other pitfalls in the evaluation of models.

It will be shown that the decomposition of models for the pressure-strain correlation into slow and rapid parts is ambiguous for uniformly strained turbulent flows where the mean velocity gradients are constant. Hence, when the commonly assumed decomposition is implemented and comparisons are made with DNS results, an overly pessimistic and misleading assessment of the performance of a pressure-strain model can be arrived at. This point is demonstrated theoretically and then is illustrated computationally by comparisons of the predictions of three recent pressure-strain models (the models of Shih and Lumley,[6] Fu, Launder and Tselepidakis[7] and Speziale, Sarkar and Gatski[8]) with the direct simulations of Rogers, Moin and Reynolds[9] for homogeneous shear flow. It will thus be argued that in uniformly strained turbulent flows, models for the pressure-strain correlation should be tested as a whole rather than tested in their slow and rapid parts. More objective alternative means for doing so will be proposed. Of course, the slow and rapid parts of models for the pressure-strain correlation can still be tested separately in the limit of relaxational turbulent flows and in the rapid distortion limit, respectively. These issues will be discussed in detail in the sections to follow.

2. ANALYSIS OF THE PRESSURE-STRAIN CORRELATION

We will base our analysis on the incompressible Navier-Stokes equations

$$\frac{\partial v_i}{\partial t} + v_j \frac{\partial v_i}{\partial x_j} = -\frac{\partial P}{\partial x_i} + \nu \nabla^2 v_i \tag{1}$$

$$\frac{\partial v_i}{\partial x_i} = 0 \tag{2}$$

where v_i is the velocity vector, P is the kinematic pressure, and ν is the kinematic viscosity of the fluid. The velocity and pressure are decomposed into ensemble mean and fluctuating parts, respectively:

$$v_i = \overline{v}_i + u_i, \quad P = \overline{P} + p. \tag{3}$$

An evolution equation for the fluctuating velocity u_i is obtained by subtracting the ensemble mean of (1) from (1) itself to yield[10]

$$\frac{\partial u_i}{\partial t} + \overline{v}_j \frac{\partial u_i}{\partial x_j} = -u_j \frac{\partial u_i}{\partial x_j} - u_j \frac{\partial \overline{v}_i}{\partial x_j} - \frac{\partial p}{\partial x_i} + \nu \nabla^2 u_i + \frac{\partial}{\partial x_j}(\overline{u_i u_j}) \tag{4}$$

which is solved subject to the incompressibility constraint

$$\frac{\partial u_i}{\partial x_i} = 0. \tag{5}$$

We will restrict our analysis to homogeneous turbulence where we have

$$\frac{\partial \overline{v}_i}{\partial x_j} = G_{ij}(t) \tag{6}$$

$$\overline{u_i u_j} = \overline{u_i u_j}(t). \tag{7}$$

Hence, for homogeneous turbulence, (4) reduces to the form

$$\frac{\partial u_i}{\partial t} + G_{jk} x_k \frac{\partial u_i}{\partial x_j} = -u_j \frac{\partial u_i}{\partial x_j} - G_{ij} u_j - \frac{\partial p}{\partial x_i} + \nu \nabla^2 u_i. \tag{8}$$

By taking the divergence of (8), the pressure can be solved for, i.e.,

$$\nabla^2 p = -2 G_{kl} \frac{\partial u_l}{\partial x_k} - \frac{\partial u_k}{\partial x_l} \frac{\partial u_l}{\partial x_k} \tag{9}$$

which, in an unbounded domain, has the general solution

$$p = \frac{1}{4\pi} \int_{-\infty}^{\infty}\int\int \frac{1}{|\mathbf{x} - \mathbf{x}^*|} \left(2 G_{kl} \frac{\partial u_l^*}{\partial x_k^*} + \frac{\partial u_k^*}{\partial x_l^*} \frac{\partial u_l^*}{\partial x_k^*} \right) d^3 x^*. \tag{10}$$

Consequently, (8) can be written as an integro-differential equation as follows:

$$\begin{aligned}\frac{\partial u_i}{\partial t} + G_{jk}x_k\frac{\partial u_i}{\partial x_j} &= -u_j\frac{\partial u_i}{\partial x_j} - G_{ij}u_j + \nu\nabla^2 u_i \\ &+\frac{1}{4\pi}\int\!\!\int\!\!\int_{-\infty}^{\infty} \frac{x_i - x_i^*}{|\mathbf{x}-\mathbf{x}^*|^3}\left(2G_{kl}\frac{\partial u_l^*}{\partial x_k^*} + \frac{\partial u_k^*}{\partial x_l^*}\frac{\partial u_l^*}{\partial x_k^*}\right) d^3x^*.\end{aligned} \tag{11}$$

When done in Fourier space, the process of obtaining Eq. (11) is equivalent to projecting the pressure out of the problem.[11]

The fluctuating pressure is decomposed into slow and rapid parts, respectively, as follows[12,13]

$$p = p^{(S)} + p^{(R)} \tag{12}$$

where the slow pressure $p^{(S)}$ and the rapid pressure $p^{(R)}$ are solutions of the Poisson equations

$$\nabla^2 p^{(S)} = -\frac{\partial u_k}{\partial x_l}\frac{\partial u_l}{\partial x_k} \tag{13}$$

$$\nabla^2 p^{(R)} = -2G_{kl}\frac{\partial u_l}{\partial x_k}. \tag{14}$$

For homogeneous turbulent flows, this decomposition is unique (for general inhomogeneous turbulent flows it is not unique due to problems with the boundary conditions). By making use of (12), the pressure-strain correlation can be decomposed into slow and rapid parts in a straightforward manner:

$$\overline{p\left(\frac{\partial u_i}{\partial x_j} + \frac{\partial u_j}{\partial x_i}\right)} = \overline{p^{(S)}\left(\frac{\partial u_i}{\partial x_j} + \frac{\partial u_j}{\partial x_i}\right)} + \overline{p^{(R)}\left(\frac{\partial u_i}{\partial x_j} + \frac{\partial u_j}{\partial x_i}\right)} \tag{15}$$

or, equivalently,

$$\Pi_{ij} = \Pi_{ij}^{(S)} + \Pi_{ij}^{(R)} \tag{16}$$

where Π_{ij} denotes the pressure-strain correlation. Here, the slow and rapid parts of the pressure-strain can be written exclusively in terms of the fluctuating velocity as follows:

$$\Pi_{ij}^{(S)} = \frac{1}{4\pi}\overline{\int\!\!\int\!\!\int_{-\infty}^{\infty} \frac{1}{|\mathbf{x}-\mathbf{x}^*|}\frac{\partial u_k^*}{\partial x_l^*}\frac{\partial u_l^*}{\partial x_k^*}\left(\frac{\partial u_i}{\partial x_j} + \frac{\partial u_j}{\partial x_i}\right) d^3x^*} \tag{17}$$

$$\Pi_{ij}^{(R)} = \frac{1}{2\pi}G_{kl}\overline{\int\!\!\int\!\!\int_{-\infty}^{\infty} \frac{1}{|\mathbf{x}-\mathbf{x}^*|}\frac{\partial u_l^*}{\partial x_k^*}\left(\frac{\partial u_i}{\partial x_j} + \frac{\partial u_j}{\partial x_i}\right) d^3x^*}. \tag{18}$$

As a direct consequence of (11), it follows that solutions of the Navier-Stokes equations for the fluctuating velocity field u_i in homogeneous turbulence are of the general form (see Appendix A)

$$u_i(\mathbf{x},t) = \mathcal{F}_i\left[G_{kl}(t');\ \mathbf{x},t\right], \quad t' \in (0,t) \tag{19}$$

where $\mathcal{F}[\,\cdot\,]$ denotes a functional (i.e., a quantity determined by the history of a function). From (19), it is clear that any moments constructed from u_i will be *nonlinear functionals* of the history of $G_{kl}(t')$. More precisely, from (17)-(18) and (19) it follows that both $\Pi_{ij}^{(S)}$ and $\Pi_{ij}^{(R)}$ can depend nonlinearly on G_{kl} at retarded times as follows:

$$\Pi_{ij}^{(S)}(t) = A_{ij}\left[G_{kl}(t');\ t\right], \quad t' \in (0,t) \tag{20}$$

$$\Pi_{ij}^{(R)}(t) = M_{ijkl}\left[G_{kl}(t');\ t\right] G_{kl}(t), \quad t' \in (0,t) \tag{21}$$

where the correlation M_{ijkl} is defined by

$$M_{ijkl} = \frac{1}{2\pi}\overline{\int_{-\infty}^{\infty}\!\!\int\!\!\int \frac{1}{|\mathbf{x}-\mathbf{x}^*|}\frac{\partial u_l^*}{\partial x_k^*}\left(\frac{\partial u_i}{\partial x_j}+\frac{\partial u_j}{\partial x_i}\right) d^3x^*}. \tag{22}$$

Here, $\Pi_{ij}^{(S)}$ and $\Pi_{ij}^{(R)}$ are functions of time alone since we are considering homogeneous turbulence for which an ensemble mean is assumed to be equivalent to a spatial average.

In the standard models for (20)-(21) that have been used in the formulation of second-order closures, explicit history effects have been neglected and the time dependence t has been parameterized through $\overline{u_iu_j}(t)$ and the dissipation rate $\varepsilon(t)$ – the only two turbulence correlations that are typically generated in the solution of these models. With these two assumptions, dimensional considerations and the fact that Π_{ij} is traceless then yields models of the form[12–14]

$$\Pi_{ij} = \varepsilon\mathcal{A}_{ij}(\mathbf{b}) + K\mathcal{M}_{ijkl}(\mathbf{b})\frac{\partial\overline{v}_k}{\partial x_l} \tag{23}$$

where

$$K = \frac{1}{2}\overline{u_iu_i} \tag{24}$$

$$\varepsilon = \nu\overline{\frac{\partial u_i}{\partial x_j}\frac{\partial u_i}{\partial x_j}} \tag{25}$$

$$b_{ij} = \frac{\overline{u_iu_j}}{2K} - \frac{1}{3}\delta_{ij} \tag{26}$$

are, respectively, the turbulent kinetic energy, the turbulent dissipation rate, and the anisotropy tensor. Due to the way in which (23) was postulated, it has become common to assume that models of this form can be decomposed into slow and rapid parts as follows:

$$\Pi_{ij}^{(S)} = \varepsilon\mathcal{A}_{ij}(\mathbf{b}) \tag{27}$$

$$\Pi_{ij}^{(R)} = K\mathcal{M}_{ijkl}(\mathbf{b})\frac{\partial\overline{v}_k}{\partial x_l}. \tag{28}$$

Certainly, (27)-(28) are consistent with the limits of relaxational and rapidly distorted turbulent flows. More precisely, in the limit of a relaxational flow where for times $t \geq 0$, we set $\partial\overline{v}_k/\partial x_l = 0$, it follows that

$$\Pi_{ij} = \Pi_{ij}^{(S)} = \varepsilon\mathcal{A}_{ij}(\mathbf{b}) \tag{29}$$

and in the rapid distortion limit where at time $t = 0$ we let $GK_0/\varepsilon_0 \to \infty$, it follows that for early elapsed times

$$\Pi_{ij} = \Pi_{ij}^{(R)} = K\mathcal{M}_{ijkl}(\mathbf{b})\frac{\partial \overline{v}_k}{\partial x_l} \tag{30}$$

given that $G \equiv \|\partial \overline{v}_k/\partial x_l\|$. However, for any uniformly strained turbulent flow where $\partial \overline{v}_k/\partial x_l$ is constant for all times, from (20) and (21) – which are a rigorous consequence of the Navier-Stokes equations – we have

$$\Pi_{ij}^{(S)} = A_{ij}\left(\frac{\partial \overline{v}_k}{\partial x_l}, t\right) \tag{31}$$

$$\Pi_{ij}^{(R)} = M_{ijkl}\left(\frac{\partial \overline{v}_m}{\partial x_n}, t\right)\frac{\partial \overline{v}_k}{\partial x_l}, \tag{32}$$

since $G_{kl}(t') = \partial \overline{v}_k/\partial x_l$. *Consequently, the decomposition of the model (23) into slow and rapid parts is unclear since both* $\Pi_{ij}^{(S)}$ *and* $\Pi_{ij}^{(R)}$ *can depend explicitly on the mean velocity gradients* $\partial \overline{v}_k/\partial x_l$. The only thing that we can say definitively is that $\varepsilon\mathcal{A}_{ij}$ is the slow pressure-strain correlation in the limit of relaxational flows and that $K\mathcal{M}_{ijkl}\partial \overline{v}_k/\partial x_l$ is the rapid pressure-strain in the rapid distortion limit.

This analysis is particularly relevant for comparison studies of existing models for the pressure-strain correlation. Many of these models have been calibrated in uniformly strained turbulent flows (i.e., homogeneous shear flow). Since for such flows, both the rapid and slow parts of the pressure-strain correlation can depend explicitly on $\partial \overline{v}_k/\partial x_l$, the implementation of the commonly assumed decomposition (27)-(28) to evaluate models can lead to misleading results as we will show more clearly in the next section.

3. COMPARISONS WITH DIRECT SIMULATIONS

Three recent models for the pressure-strain correlation will be compared with the direct simulations of Rogers, Moin and Reynolds[9] for homogeneous shear flow. These models are as follows:

Shih-Lumley Model (SL)

$$\begin{aligned}
\Pi_{ij} \;=\; & -\beta\varepsilon b_{ij} + \frac{4}{5}K\overline{S}_{ij} + 12\alpha_5 K\left(b_{ik}\overline{S}_{jk} + b_{jk}\overline{S}_{ik}\right. \\
& \left. -\frac{2}{3}b_{kl}\overline{S}_{kl}\delta_{ij}\right) + \frac{4}{3}(2-7\alpha_5)K(b_{ik}\overline{W}_{jk} + b_{jk}\overline{W}_{ik}) \\
& +\frac{4}{5}K(b_{il}b_{lm}\overline{S}_{jm} + b_{jl}b_{lm}\overline{S}_{im} - 2b_{ik}\overline{S}_{kl}b_{lj} \\
& -3b_{kl}\overline{S}_{kl}b_{ij}) + \frac{4}{5}K(b_{il}b_{lm}\overline{W}_{jm} + b_{jl}b_{lm}\overline{W}_{im})
\end{aligned} \tag{33}$$

where

$$\beta = 2 + \frac{F}{9}\exp(-7.77/\sqrt{Re_t})\{72/\sqrt{Re_t} + 80.1\ ln[1 + 62.4(-II + 2.3III)]\} \tag{34}$$

$$F = 1 + 9II + 27III \tag{35}$$

$$II = -\frac{1}{2}b_{ij}b_{ij}, \quad III = \frac{1}{3}b_{ij}b_{jk}b_{ki} \tag{36}$$

$$Re_t = \frac{4}{9}\frac{K^2}{\nu\varepsilon} \tag{37}$$

$$\alpha_5 = \frac{1}{10}\left(1 + \frac{4}{5}F^{\frac{1}{2}}\right) \tag{38}$$

Fu, Launder and Tselepidakis Model (FLT)

$$\begin{aligned}\Pi_{ij} &= 120II\sqrt{F}\varepsilon\left[b_{ij} + 1.2\left(b_{ik}b_{kj} - \frac{1}{3}b_{kl}b_{kl}\delta_{ij}\right)\right] \\ &+\frac{4}{5}K\overline{S}_{ij} + 1.2K\left(b_{ik}\overline{S}_{jk} + b_{jk}\overline{S}_{ik} - \frac{2}{3}b_{kl}\overline{S}_{kl}\delta_{ij}\right) \\ &+\frac{26}{15}K(b_{ik}\overline{W}_{jk} + b_{jk}\overline{W}_{ik}) + \frac{4}{5}K(b_{ik}b_{kl}\overline{S}_{jl} \\ &+b_{jk}b_{kl}\overline{S}_{il} - 2b_{ik}\overline{S}_{kl}b_{lj} - 3b_{kl}\overline{S}_{kl}b_{ij}) \\ &+\frac{4}{5}K\left(b_{ik}b_{kl}\overline{W}_{jl} + b_{jk}b_{kl}\overline{W}_{il}\right) - \frac{14}{5}K\left[8II(b_{ik}\overline{W}_{jk}\right. \\ &\left.+b_{jk}\overline{W}_{ik}\right) + 12\left(b_{ik}b_{kl}\overline{W}_{lm}b_{mj} + b_{jk}b_{kl}\overline{W}_{lm}b_{mi}\right)\Big]\end{aligned} \tag{39}$$

Speziale, Sarkar and Gatski Model (SSG)

$$\begin{aligned}\Pi_{ij} &= -(C_1\varepsilon + C_1^*\mathcal{P})b_{ij} + C_2\varepsilon\left(b_{ik}b_{kj} - \frac{1}{3}b_{kl}b_{kl}\delta_{ij}\right) + (C_3 - C_3^*II_b^{\frac{1}{2}})K\overline{S}_{ij} \\ &+C_4K\left(b_{ik}\overline{S}_{jk} + b_{jk}\overline{S}_{ik} - \frac{2}{3}b_{kl}\overline{S}_{kl}\delta_{ij}\right) + C_5K(b_{ik}\overline{W}_{jk} + b_{jk}\overline{W}_{ik})\end{aligned} \tag{40}$$

where $\mathcal{P} = -\overline{u_iu_j}\partial\overline{v}_i/\partial x_j$ is the turbulence production and

$$C_1 = 3.4,\ C_1^* = 1.80,\ C_2 = 4.2 \tag{41}$$

$$C_3 = \frac{4}{5},\ C_3^* = 1.30,\ C_4 = 1.25 \tag{42}$$

$$C_5 = 0.40,\ II_b = b_{ij}b_{ij} \tag{43}$$

(see Shih and Lumley,[6] Fu, Launder and Tselepidakis[7] and Speziale, Sarkar and Gatski[8] for more details). In (33) and (39)-(40) $\overline{S}_{ij}$ and $\overline{W}_{ij}$ are, respectively, the symmetric and antisymmetric parts of the mean velocity gradient tensor $\partial\overline{v}_i/\partial x_j$ which are given by

$$\overline{S}_{ij} = \frac{1}{2}\left(\frac{\partial\overline{v}_i}{\partial x_j} + \frac{\partial\overline{v}_j}{\partial x_i}\right) \tag{44}$$

$$\overline{W}_{ij} = \frac{1}{2}\left(\frac{\partial\overline{v}_i}{\partial x_j} - \frac{\partial\overline{v}_j}{\partial x_i}\right) \tag{45}$$

The values of the pressure-strain correlation computed in the direct simulations of Rogers, Moin and Reynolds[9] for homogeneous shear flow will be compared with the predictions of the SL, FLT and SSG models. Here the latter are obtained by substituting the DNS values for $b_{ij}, \partial\overline{v}_i/\partial x_j, K$ and ε into (33)-(43) where, in homogeneous shear flow, the mean velocity gradient tensor takes the form

$$\frac{\partial\overline{v}_i}{\partial x_j} = \begin{pmatrix} 0 & S & 0 \\ 0 & 0 & 0 \\ 0 & 0 & 0 \end{pmatrix} \tag{46}$$

given that S is the shear rate. Comparisons will be made with the DNS for $t^* \equiv St \geq 2$ which corresponds to $\varepsilon_0 t/K_0 > 1$. An eddy turnover time is allowed for the artificial early transient effects to die out (the shear is turned on at time $t = 0$ when the turbulence consists of a random isotropic velocity field with a square-pulse energy spectrum). Since S is constant, this DNS constitutes a uniformly strained turbulent flow as discussed in the previous section.

In Figures 1(a)-(c) the predictions of the models for the slow pressure-strain correlation – based on the commonly assumed decomposition (27) – are compared with the DNS results of Rogers et al.[9] for homogeneous shear flow (run C128U). From these results it would appear that the SL model is far superior to the FLT and SSG models insofar as the modeling of slow pressure-strain correlation is concerned. Similarly, in Figures 2(a)-(c) the predictions of the SL, FLT and SSG models for the rapid pressure-strain correlation based on the decomposition (28) are compared with the same DNS test case.[9] Again, one is tempted to draw the same conclusion about the superiority of the SL model in comparison to the FLT and SSG models. However, when the model predictions for the total pressure-strain correlation are compared with the same DNS data, a rather different picture emerges. In Figures 3(a)-(c) the predictions of the SL, FLT and SSG models are compared with the DNS results for the total pressure-strain. Here, the model predictions are in much closer proximity to one another and the relative superiority of the performance of the models is less clear. The SL model is in the closest agreement with the DNS data for Π_{11}; the SSG model does the best for the Π_{12} component; and the results are mixed for the Π_{22} component although FLT and SL are on balance better than SSG. From these results it is impossible to judge which of

the models has better predictive capabilities. The examination of other test cases from this DNS data base is of little help. For example, the same type of mixed results are obtained from the C128X run of Rogers et al.[9] (see Figures 4(a)-(c)).

It is now clear that for homogeneous shear flow the direct comparison of these independent models for the pressure-strain correlation with DNS results for Π_{ij} is not very illuminating. Furthermore, as shown by the analysis in Section 2, since the decomposition of models for the pressure-strain correlation into slow and rapid parts is ambiguous in homogeneous shear flow, highly misleading conclusions can be drawn when comparisons are made exclusively based on the decompositions. A few further comments are in order concerning the implications of this point for turbulence modeling. It could be argued that since many of the authors who have developed models for the pressure strain correlation have utilized the decompositions (27)-(28) in the derivation of their models, then why is it unsound in these cases to compare the parts of the model separately? It must be remembered that the rapid parts of these models have usually not been calibrated separately. Namely, uniform shear flow results have typically been used to calibrate the "rapid" part of the model *after* the "slow" part was calibrated based on the return to isotropy problem. Since, in uniform shear flow, both the slow and rapid parts of the pressure-strain correlation depend explicitly on the mean velocity gradients as shown in (31)-(32), it follows that, when calibrated in this fashion, the model (28) ends up accounting for both the rapid pressure-strain correlation and the strain-dependent part of the slow pressure-strain correlation. This could explain why these models do not perform well in the rapid distortion limit (see Reynolds[15]).

While the Shih-Lumley model appears to yield slow and rapid parts that compare well with DNS data for homogeneous shear flow as shown in Figures 1-2, this agreement is fortuitous. For other homogeneous turbulent flows, the agreement of the individual parts of the model is not nearly so favorable. In Figures 5(a)-(c) the components of the slow pressure-strain correlation predicted by the SL, FLT and SSG models are compared with the DNS data of Rogallo[2] for plane strain. It is clear from these results that none of the models are able to yield results in close range of this DNS. Similar negative results were recently reported by Shih et al.[3] for the axisymmetric expansion as well as for plane strain turbulence. It is thus clear that this commonly adopted practice of testing the "slow" and "rapid" parts of the pressure-strain correlation in homogeneously strained turbulent flows should be abandoned in favor of alternative tests based on the total pressure-strain correlation. This point led the present authors to model the total pressure-strain correlation, without using the decompositions (27)-(28), when formulating the SSG model. Such an approach had been proposed previously by Leslie.[16] It must be remembered that only the *total* pressure-strain correlation enters into the Reynolds stress transport equation.

4. ALTERNATIVE TESTS OF PRESSURE-STRAIN MODELS USING DNS

As shown in the last section, the direct comparison of models for the pressure-strain correlation with DNS can be either misleading or inconclusive. The only way to obtain a more accurate gauge on the performance of pressure-strain models in homogeneously strained turbulent flows is to compute these flows with a full second-order closure that incorporates these models and then compare with DNS results. In this way, the ability of these models to yield good predictions for the time evolution of the Reynolds stresses as well as the equilibrium anisotropies can be assessed. In the final analysis, the purpose of these pressure-strain models is to yield a full Reynolds stress closure; hence, such models should be judged good or bad based on their ability to yield accurate predictions for the Reynolds stresses.

The Reynolds stress transport equation takes the form[10]

$$\dot{\overline{u_i u_j}} = -\overline{u_i u_k}\frac{\partial \overline{v}_j}{\partial x_k} - \overline{u_j u_k}\frac{\partial \overline{v}_i}{\partial x_k} + \Pi_{ij} - \varepsilon_{ij} \tag{47}$$

for homogeneous turbulence. Consequently, in order to achieve closure, a model for the turbulent dissipation rate tensor ε_{ij} is needed in addition to a model for the pressure-strain correlation Π_{ij}. This does cause some concern since inaccurate model predictions can arise from two sources: the pressure-strain correlation or the dissipation rate tensor. However, in virtually all of the commonly used second-order closures, the turbulent dissipation rate ε is modeled as follows:

$$\dot{\varepsilon} = -C_{\varepsilon 1}\frac{\varepsilon}{K}\overline{u_i u_j}\frac{\partial \overline{v}_i}{\partial x_j} - C_{\varepsilon 2}\frac{\varepsilon^2}{K} \tag{48}$$

in homogeneous turbulence where $\varepsilon \equiv \frac{1}{2}\varepsilon_{ii}$ and $C_{\varepsilon 1}$ and $C_{\varepsilon 2}$ are either constants or functions of II, III and Re_t. This model - which has its origins in the work of Davidov[17] and Launder and co-workers[18-19] - has been shown recently by Speziale and Mac Giolla Mhuiris[20] to perform well in homogeneous shear flow. Hence, if versions of (48) that are compatible with the SL, FLT and SSG models are chosen, a fair basis of comparison is established between these pressure strain models. The form of the coefficients chosen by SL, FLT and SSG are as follows:

Shih and Lumley Model

$$C_{\varepsilon 1} = 1.2,\ C_{\varepsilon 2} = \frac{7}{5} + 0.49\exp(-2.83 Re_t^{-\frac{1}{2}})[1 - 0.33 ln(1 - 55II)] \tag{49}$$

Fu, Launder and Tselepidakis Model

$$C_{\varepsilon 1} = 1.45,\ C_{\varepsilon 2} = 1.90 \tag{50}$$

Speziale, Sarkar and Gatski Model

$$C_{\epsilon 1} = 1.44, \; C_{\epsilon 2} = 1.83. \tag{51}$$

The effect of variations of these coefficients will be discussed briefly later. Both the SL and SSG models are used with Kolmogorov's assumption of local isotropy

$$\varepsilon_{ij} = \frac{2}{3}\varepsilon\delta_{ij}. \tag{52}$$

In the FLT model, a simple algebraic model is used to parameterize the anisotropy of dissipation as follows:

$$\varepsilon_{ij} = \frac{2}{3}\varepsilon\sqrt{F}\delta_{ij} + (1-\sqrt{F})\frac{\varepsilon}{K}\overline{u_i u_j} \tag{53}$$

wherein ε is obtained from (48). This model is needed for consistency with the limit of two-component turbulence (in more recent versions of the model of Launder and co-workers, the anisotropic part of (53) is combined with Π_{ij}).

Now, computations of the Reynolds stresses predicted by the models will be compared with the DNS results of Rogers et al.[9] for homogeneous shear. In Figure 6, the predictions of the SL, FLT and SSG models for the time evolution of the turbulent kinetic energy are compared with run C128W of the DNS[9] (here, $K^* = K/K_0$, $t^* = St$). These results appear to indicate that the SL model performs the best, by far. Shih et al.[3] reported very similar results for the SL model for run C128W of the DNS which they used to argue for the superiority of this model. However, it becomes clear that these good results are fortuitous when other cases are considered. In Figures 7-8, the model predictions are compared with DNS results for runs C128U and C128X of Rogers et al.[9] For these cases, none of the models are able to predict the trends of the DNS. The reason for this is that the initial conditions of the DNS are contaminated. More specifically at time $t^* = 0$ when the shear is turned on, the flow is seeded with a random isotropic velocity field with a square pulse spectrum (see Rogallo[2]). Hence it is unrealistic to expect one-point turbulence models to predict the early time evolution of this "pseudo-turbulence" (the artificial nature of the early transient is best illustrated by run C128X shown in Figure 8 for which the turbulence Reynolds number drops an order of magnitude during the first eddy turnover time). At least one eddy turnover should be allowed to elapse before making comparisons; this corresponds to

$$\frac{\varepsilon_0 t}{K_0} > 1$$

or $St \geq 2$ for the initial conditions of these simulations. Hence at $St = 2$, the values of $\overline{u_i u_j}$ and ε taken from the DNS – which correspond to a more physical turbulence with a developed energy spectrum – are now used as initial conditions for the models. With these

more physical initial conditions, a different picture emerges. For the C128W run shown in Figure 9(a) the SSG model now yields the best predictions in comparison to the DNS results. For the C128U run shown in Figure 9(b), the FLT model performs the best; whereas for the C128X run shown in Figure 9(c) the FLT and SSG models perform comparably well. However, in all of these runs, the SL model performs poorly. This is due to its underprediction of the growth rate – a result that will be shown later. By basing the calculations on the contaminated initial conditions at $St = 0$, it would be erroneously concluded that the SL model performs the best among these models in homogeneous shear flow.

Finally, we will provide a much more reliable criterion for judging the predictive capabilities of pressure-strain models in homogeneous shear flow. All of these models predict that when an initially isotropic turbulence is suddenly subjected to a mean strain then, during the early times,

$$\Pi_{ij} \approx \frac{4}{5} K \overline{S}_{ij}. \tag{54}$$

This result was first derived by Crow[21]; it is a rigorous constraint that can be obtained by simple symmetry arguments. Eq. (54) guarantees that the models will perform well for early times. Hence, the prospect that the models will perform well at later times is tied strongly to their ability to predict the equilibrium values $(b_{ij})_\infty$ and $(SK/\varepsilon)_\infty$ since these are approached within a few eddy turnover times and achieve values that are independent of the initial conditions – a feature that is universal in homogeneous shear flow.[20] In Table 1, the equilibrium values predicted by the SL, FLT and SSG models for homogeneous shear flow are compared with the DNS results of Rogers et al.[9] averaged over the six runs discussed therein. Here,

$$\left(\frac{\mathcal{P}}{\varepsilon}\right)_\infty = -2(b_{12})_\infty \left(\frac{SK}{\varepsilon}\right)_\infty \tag{55}$$

is the equilibrium value of the ratio of production to dissipation and

$$\lambda_\infty = -2(b_{12})_\infty - \left(\frac{\varepsilon}{SK}\right)_\infty \tag{56}$$

is the equilibrium growth rate (for $t^* \gg 1$, $K^*, \varepsilon^* \sim e^{\lambda_\infty t^*}$). It now becomes clear why the FLT and SSG models perform more favorably compared to the DNS results of Rogers et al.[9] Both FLT and SSG yield growth rates that are in the range of the DNS; similarly the other equilibrium values are close to the DNS results. However, the SL model yields equilibrium values for b_{ij} and SK/ε which – with the exception of $(b_{11})_\infty$ – compare poorly with the DNS results as shown in Table 1. In particular, the growth rate λ_∞ is underpredicted by 20%: a result which explains why the SL model predictions are consistently below the DNS data for the turbulent kinetic energy shown in Figures 9(a)-(c) for three independent cases. Similar conclusions can be drawn when comparisons are made with the independent large-eddy simulation of Bardina et al.[22] shown in Figure 10.

Some comments are in order concerning the effect of the model constants in (48) on the performance of the SL model. For example, could the bad predictions of the SL model be due to problems with the modeled dissipation rate transport equation? The answer to this question appears to be no. Shih (private communication) has used a variety of values for $C_{\varepsilon 1}$ in the range of $1 \leq C_{\varepsilon 1} \leq 1.25$ for the calculation of homogeneous turbulent flows (for homogeneous shear flow, Shih et al.[3] used a value of $C_{\varepsilon 1} \approx 1.2$ which prompted us to use the same value for the calculations presented herein). It can be shown that $C_{\varepsilon 1} = 1$ constitutes a bifurcation point of the ε-transport equation where $(SK/\varepsilon)_\infty \to \infty$ and the exponential growth of K and ε is replaced with an algebraic growth (see Speziale[23]). Hence, a significant reduction of $C_{\varepsilon 1}$ below 1.2 will further degrade the already bad prediction of $(SK/\varepsilon)_\infty$ made by the SL model (see Table 1) and bring the model dangerously close to the bifurcation point $C_{\varepsilon 1} = 1$. Larger values of $C_{\varepsilon 1}$ alleviate the bad predictions for $(SK/\varepsilon)_\infty$ and $(\mathcal{P}/\varepsilon)_\infty$. Speziale et al.[24] computed homogeneous shear flow for the SL model using the more traditional value of $C_{\varepsilon 1} = 1.44$. This calculation yields $(SK/\varepsilon)_\infty \approx 7$ and $(\mathcal{P}/\varepsilon)_\infty \approx 1.7$ which are much better; however, it was at the expense of the growth rate λ_∞ which drops to 0.09 – a value which would even further lower the predictions of the SL model in comparison to the DNS results of Rogers et al.[9] shown in Figures 9(a)-(c). Furthermore, for $C_{\varepsilon 1} > 1.4$ the maximum anisotropy $(b_{11})_\infty$ drops to only approximately one-half of the value shown in Table 1 – a serious underprediction.[24] Hence, it is clear that there is no value of $C_{\varepsilon 1}$ which will render good predictions for the SL model in homogeneous shear flow. Since $C_{\varepsilon 1}$ and $C_{\varepsilon 2}$ only enter into the prediction of the equilibrium values through the combination[20]

$$\frac{C_{\varepsilon 2} - 1}{C_{\varepsilon 1} - 1} = \left(\frac{\mathcal{P}}{\varepsilon}\right)_\infty \tag{57}$$

(which should be approximately 1.8), only $C_{\varepsilon 1}$ needs to be varied. It therefore follows that it is not possible for the SL model to yield good results for homogeneous shear flow when used in conjunction with a modeled dissipation rate transport equation of the standard form (48).

Of course, these results raise the question as to why the SL model performs so poorly yet appears to be so favorable in comparison to the DNS data of Rogers et al.[9] for the pressure strain correlation (see Figures 3(a)-(c)). A possible explanation arises from Figure 3(b) for the crucial Π_{12} component which contributes strongly to the determination of the growth rate.[20] By the end of the simulation, the SL model predictions are diverging away from the DNS data whereas the FLT and SSG model predictions are converging toward the DNS data.

5. CONCLUDING REMARKS

Considerable care must be exercised when DNS data bases are used to evaluate the

performance of turbulence models. The recent practice of comparing separately the model predictions for the "slow" and "rapid" parts of the pressure-strain correlation with DNS data bases for homogeneously strained turbulent flows is fundamentally unsound. This is due to the fact that the decomposition of models for the pressure-strain correlation into slow and rapid parts is ambiguous in such flows since both parts can depend explicitly on the mean velocity gradients. As a result of the way in which models for the pressure-strain correlation are calibrated, the part of the model that depends explicitly on the mean velocity gradients is actually accounting for contributions from both the slow and rapid terms in these flows. Consequently, when a model is decomposed into slow and rapid parts along the traditional lines (27)-(28), highly misleading results can be obtained when separate comparisons are made with DNS results for the slow and rapid pressure strain correlations drawn from homogenous shear flow.

The individual slow and rapid parts of the commonly used models can only be properly tested in the limit of relaxational flows and in the rapid distortion limit, respectively. None of these models are consistent with DNS or RDT in the rapid distortion limit as recently demonstrated by Reynolds[15] – a deficiency which in all likelihood arises from the neglect of the nonlinear history effects in (20)-(21). Evidence is rapidly accumulating that models of the commonly assumed form (23) cannot accommodate both the rapid distortion and moderately strained flow limits. Other pitfalls can be encountered when DNS data bases are used to test pressure-strain models in the limit of relaxational flows (i.e., the return to isotropy problem). The DNS data bases of Lee and Reynolds[25] that are typically used are for Reynolds numbers $Re_\lambda < 10$ based on the Taylor microscale. At such low Reynolds numbers there is virtually no return to isotropy – an effect that can only be captured by pressure-strain models where the Rotta coefficient goes to 2 as Re_λ becomes of $O(1)$. Consequently, it is not surprising that the SL model – which has just such a low Reynolds number correction – performs better than the high Reynolds number SSG and FLT models in these relaxational flows as shown by Shih and Lumley.[5] However, when high Reynolds number experiments are considered, a drastically different picture emerges as shown recently by Sarkar and Speziale[26] (here, the SSG model performed better than the SL model in three out of four experimental test cases of the return to isotropy problem at higher Reynolds numbers).

In the final analysis, simplified models for the pressure-strain correlation such as (23) are primarily useful in so far as they are able to render reliable predictions for the Reynolds stresses within the framework of an otherwise internally consistent second-order closure. For homogeneous turbulence this is best achieved by satisfying the Crow[21] constraint and by calibrating the model to yield good equilibrium values for the Reynolds stress anisotropies in benchmark cases like homogeneous shear flow (the former ensures good predictions for

early times whereas the latter enhances the prospects for good predictions at later times). The FLT and SSG models discussed in this paper perform much better than the SL model in homogeneous shear flow since the former two models were partially calibrated based on experimental data for this flow. On the other hand, the SL model was largely formulated based on the satisfaction of the constraint of realizability in the limit of two-component turbulence. The formulation of models exclusively by the satisfaction of an extreme constraint – exact as it may be – may not guarantee that a model will perform well in basic benchmark flows. Deficiencies like those uncovered in this study can be overlooked when models for the pressure-strain correlation are compared in isolation with DNS data bases without a direct examination of their predictive capabilities within the framework of a full Reynolds stress closure.

REFERENCES

[1]P. Moin, W. C. Reynolds and J. Kim, eds., "Studying Turbulence Using Numerical Simulation Databases," *Proceedings of the 1987 Summer Program of the Center for Turbulence Research*, Stanford University Press (1987).

[2]R. S. Rogallo, "Numerical Experiments in Homogeneous Turbulence," *NASA Technical Memorandum 81315* (1981).

[3]T. H. Shih, N. N. Mansour and J. Y. Chen, "Reynolds Stress Models of Homogeneous Turbulence," in *Proceedings of the 1987 Summer Program of the Center for Turbulence Research*, (P. Moin et al., eds.), p. 191, Stanford University Press (1987).

[4]J. Weinstock and K. Shariff, "Evaluation of a Theory for Pressure-Strain Rate," in *Proceedings of the 1987 Summer Program of the Center for Turbulence Research*, (P. Moin et al., eds.), p. 213, Stanford University Press (1987).

[5]T. H. Shih and J. L. Lumley, "A Critical Comparison of Second-Order Closures with Direct Numerical Simulation of Homogeneous Turbulence," *NASA Technical Memorandum 105351*, ICOMP, NASA Lewis Research Center (1991).

[6]T. H. Shih and J. L. Lumley, "Modeling of Pressure Correlation Terms in Reynolds Stress and Scalar Flux Equations," *Cornell University Technical Report FDA-85-3* (1985).

[7]S. Fu, B. E. Launder and D. P. Tselepidakis, "Accommodating the Effects of High Strain Rates in Modeling the Pressure-Strain Correlation," *UMIST Technical Report TFD/87/5* (1987).

[8]C. G. Speziale, S. Sarkar and T. B. Gatski, "Modeling the Pressure-Strain Correlation of Turbulence: An Invariant Dynamical Systems Approach," *J. Fluid Mech.* **227**, 245 (1991).

[9]M. M. Rogers, P. Moin and W. C. Reynolds, "The Structure and Modeling of the Hydrodynamic and Passive Scalar Fields in Homogeneous Turbulent Shear Flow," *Stanford University Technical Report TF-25* (1986).

[10]J. O. Hinze, *Turbulence* (McGraw-Hill, New York, 1975).

[11]M. Lesieur, *Turbulence in Fluids* (Martinus Nijhoff, Boston, 1990).

[12]W. C. Reynolds, "Fundamentals of Turbulence for Turbulence Modeling and Simulation," *Lecture Notes for Von Kármán Institute, AGARD Report No. 755* (NATO, Specialized Printing Services, Loughton, Essex, 1987).

[13]J. L. Lumley, "Computational Modeling of Turbulent Flows," *Adv. Appl. Mech.* **18**, 123 (1978).

[14]C. G. Speziale, "Analytical Methods for the Development of Reynolds Stress Closures in Turbulence," *Ann. Rev. Fluid Mech.* **23**, 107 (1991).

[15]W. C. Reynolds, "Effects of Rotation on Homogeneous Turbulence," *Proc. 10th Australasian Fluid Mech. Conf.*, University of Melbourne, pp. 1-6 (1989).

[16]D. C. Leslie, "Analysis of a Strongly Sheared, Nearly Homogeneous Turbulent Shear Flow," *J. Fluid Mech.* **98**, 435 (1980).

[17]B. I. Davidov, "Statistical Dynamics of an Incompressible Turbulent Fluid," *Dokl. Akad Nauk SSSR* **136**, 47 (1961).

[18]K. Hanjalic and B. E. Launder, "A Reynolds Stress Model of Turbulence and its Application to Thin Shear Flows," *J. Fluid Mech.* **52**, 609 (1972).

[19]B. E. Launder and D. B. Spalding, "The Numerical Computation of Turbulent Flows," *Comput. Methods Appl. Mech. Eng.* **3**, 269 (1974).

[20]C. G. Speziale and N. Mac Giolla Mhuiris, "On the Prediction of Equilibrium States in Homogeneous Turbulence," *J. Fluid Mech.* **209**, 591 (1989).

[21]S. C. Crow, "Viscoelastic Properties of Fine-Grained Incompressible Turbulence," *J. Fluid Mech.* **33**, 1 (1968).

[22]J. Bardina, J. H. Ferziger and W. C. Reynolds, "Improved Turbulence Models Based on Large-Eddy Simulation of Homogeneous Incompressible Turbulent Flows," *Stanford University Technical Report TF-19* (1983).

[23]C. G. Speziale, "Discussion of Turbulence Modeling: Present and Future," *Proc. Whither Turbulence Workshop, Lecture Notes in Phys.* **357** (J. L. Lumley, ed.), p. 490 (1990).

[24]C. G. Speziale, T. B. Gatski and N. Mac Giolla Mhuiris, "A Critical Comparison of Turbulence Models for Homogeneous Turbulent Shear Flows in a Rotating Frame," *Phys. Fluids A* **2**, 1678 (1990).

[25]M. J. Lee and W. C. Reynolds, "Numerical Experiments on the Structure of Homogeneous Turbulence," *Stanford University Technical Report TF-24* (1985).

[26]S. Sarkar and C. G. Speziale, "A Simple Nonlinear Model for the Return to Isotropy in Turbulence," *Phys. Fluids A* **2**, 84 (1990).

APPENDIX A

The equation of motion (11) for the fluctuating velocity can be rewritten in the alternative form

$$\begin{aligned}\frac{\partial u_i}{\partial t} - \nu\nabla^2 u_i &= -u_j\frac{\partial u_i}{\partial x_j} - G_{jk}x_k\frac{\partial u_i}{\partial x_j} - G_{ij}u_j \\ &+\frac{1}{4\pi}\int_{-\infty}^{\infty}\!\!\int\!\!\int \frac{x_i - x_i^*}{|\mathbf{x}-\mathbf{x}^*|^3}\left(2G_{kl}\frac{\partial u_l^*}{\partial x_k^*} + \frac{\partial u_k^*}{\partial x_l^*}\frac{\partial u_l^*}{\partial x_k^*}\right) d^3x^*\end{aligned} \tag{A1}$$

for any homogeneous turbulent flow. By making use of the Green's function for the diffusion operator, (A1) can be converted to the equivalent form

$$\begin{aligned}u_i(\mathbf{x},t) &= -\frac{1}{4\pi\nu}\int_0^t \int_{-\infty}^{\infty}\!\!\int\!\!\int H(\mathbf{x}-\mathbf{x}',t-t')\left[u_j'\frac{\partial u_i'}{\partial x_j'} + G_{jk}(t')x_k'\frac{\partial u_i'}{\partial x_j'}\right. \\ &+G_{ij}(t')u_j' - \frac{1}{4\pi}\int_{-\infty}^{\infty}\!\!\int\!\!\int \frac{x_i - x_i^*}{|\mathbf{x}-\mathbf{x}^*|^3}\left(2G_{kl}(t')\frac{\partial u_l^*(t')}{\partial x_k^*}\right. \\ &\left.\left.+\frac{\partial u_k^*(t')}{\partial x_l^*}\frac{\partial u_l^*(t')}{\partial x_k^*}\right) d^3x^*\right] d^3x'dt' \\ &+\frac{1}{4\pi\nu}\int_{-\infty}^{\infty}\!\!\int\!\!\int H(\mathbf{x}-\mathbf{x}',t)u_i(\mathbf{x}',0)d^3x'\end{aligned} \tag{A2}$$

where

$$H(\mathbf{x}-\mathbf{x}',t-t') = \frac{1}{2\sqrt{\pi\nu}(t-t')^{\frac{3}{2}}}\exp\left[-|\mathbf{x}-\mathbf{x}'|^2/4\nu(t-t')\right] \tag{A3}$$

is the Green's function which is non-zero only for $t - t' > 0$. For an ensemble of initial conditions $u_i(\mathbf{x},0)$, one could envision solving (A2) iteratively. These solutions would be of the general mathematical form

$$u_i(\mathbf{x},t) = \mathcal{F}_i[G_{kl}(t');\mathbf{x},t], \quad t' \in (0,t) \tag{A4}$$

where $\mathcal{F}_i[\,\cdot\,]$ denotes a functional in the history of the mean velocity gradient tensor G_{kl}. Consequently, the fluctuating velocity – as well as any statistics constructed from it – will depend nonlinearly on the history of the mean velocity gradients. On physical grounds, the duration of this history dependence would be expected to be of the order of an eddy turnover time.

Equilibrium Values	SL Model	FLT Model	SSG Model	DNS Results
$(b_{11})_\infty$	0.202	0.208	0.204	0.215
$(b_{12})_\infty$	–0.081	–0.146	–0.156	–0.158
$(b_{22})_\infty$	–0.195	–0.144	–0.148	–0.153
$(b_{33})_\infty$	–0.007	–0.064	–0.056	–0.062
$(SK/\varepsilon)_\infty$	21.3	6.84	5.98	5.70
$(\mathcal{P}/\varepsilon)_\infty$	3.43	2.00	1.87	1.80
λ_∞	0.114	0.146	0.145	0.14

Table 1. Comparison of the equilibrium values predicted by the SL, FLT and SSG models with the DNS results of Rogers et al.[9] for homogeneous shear flow.

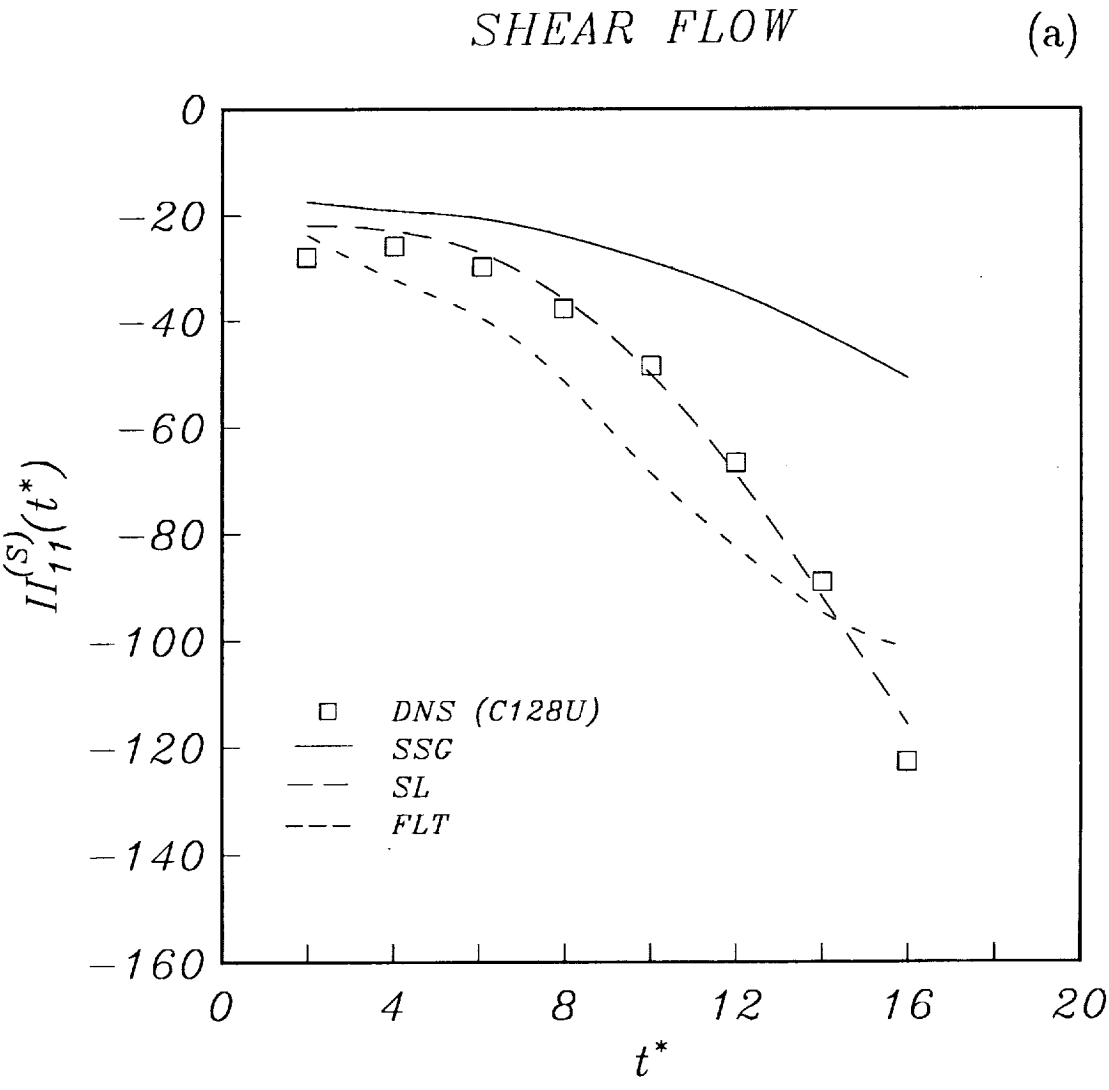

Figure 1. Comparison of the predictions of the SL, FLT and SSG models for the "slow" pressure-strain correlation with the DNS results of Rogers et al.[9] for homogeneous shear flow (run C128U). (a) $\Pi_{11}^{(S)}$ component, (b) $\Pi_{12}^{(S)}$ component, and (c) $\Pi_{22}^{(S)}$ component.

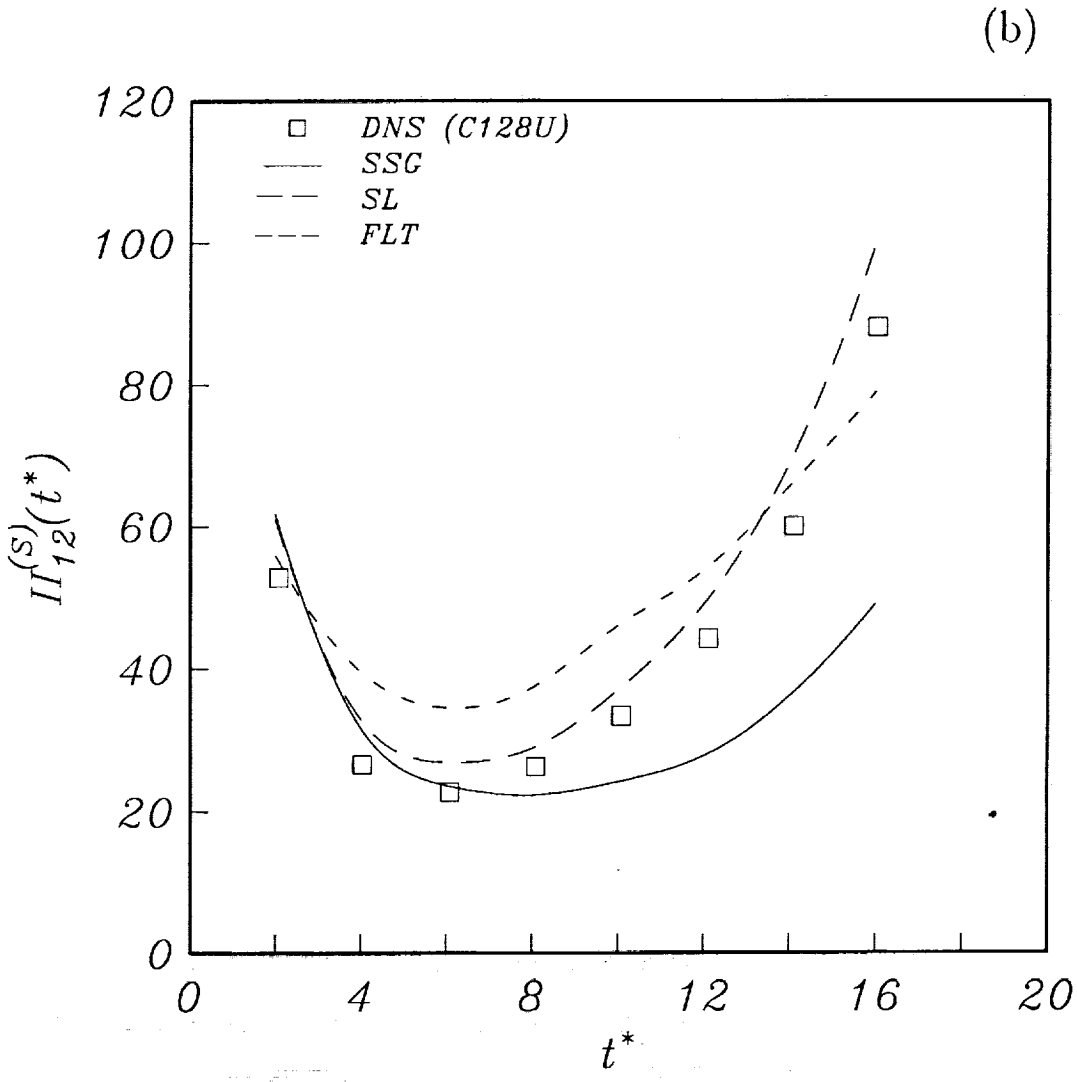

Figure 1. Comparison of the predictions of the SL, FLT and SSG models for the "slow" pressure-strain correlation with the DNS results of Rogers et al.[9] for homogeneous shear flow (run C128U). (a) $\Pi_{11}^{(S)}$ component, (b) $\Pi_{12}^{(S)}$ component, and (c) $\Pi_{22}^{(S)}$ component.

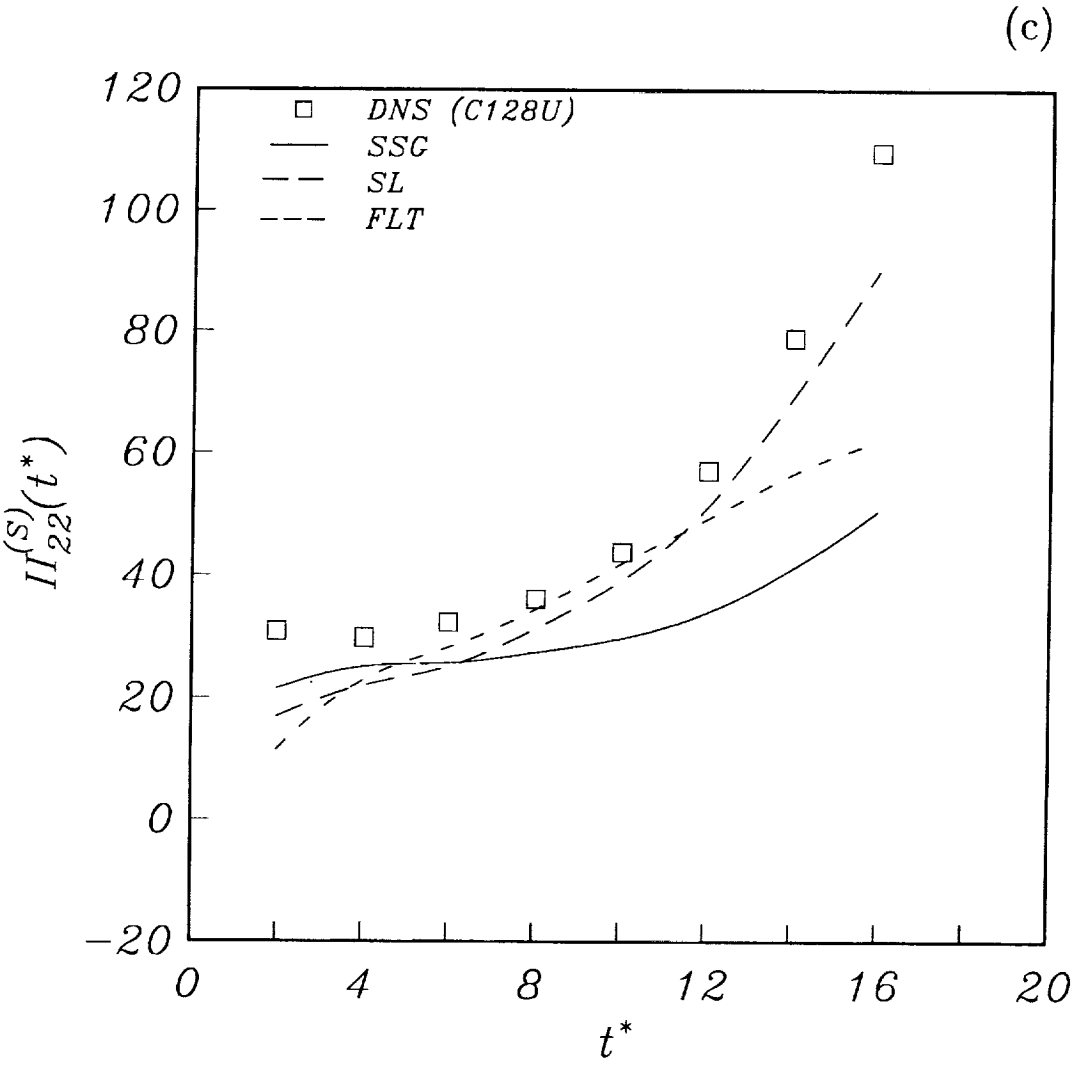

Figure 1. Comparison of the predictions of the SL, FLT and SSG models for the "slow" pressure-strain correlation with the DNS results of Rogers et al.[9] for homogeneous shear flow (run C128U). (a) $\Pi_{11}^{(S)}$ component, (b) $\Pi_{12}^{(S)}$ component, and (c) $\Pi_{22}^{(S)}$ component.

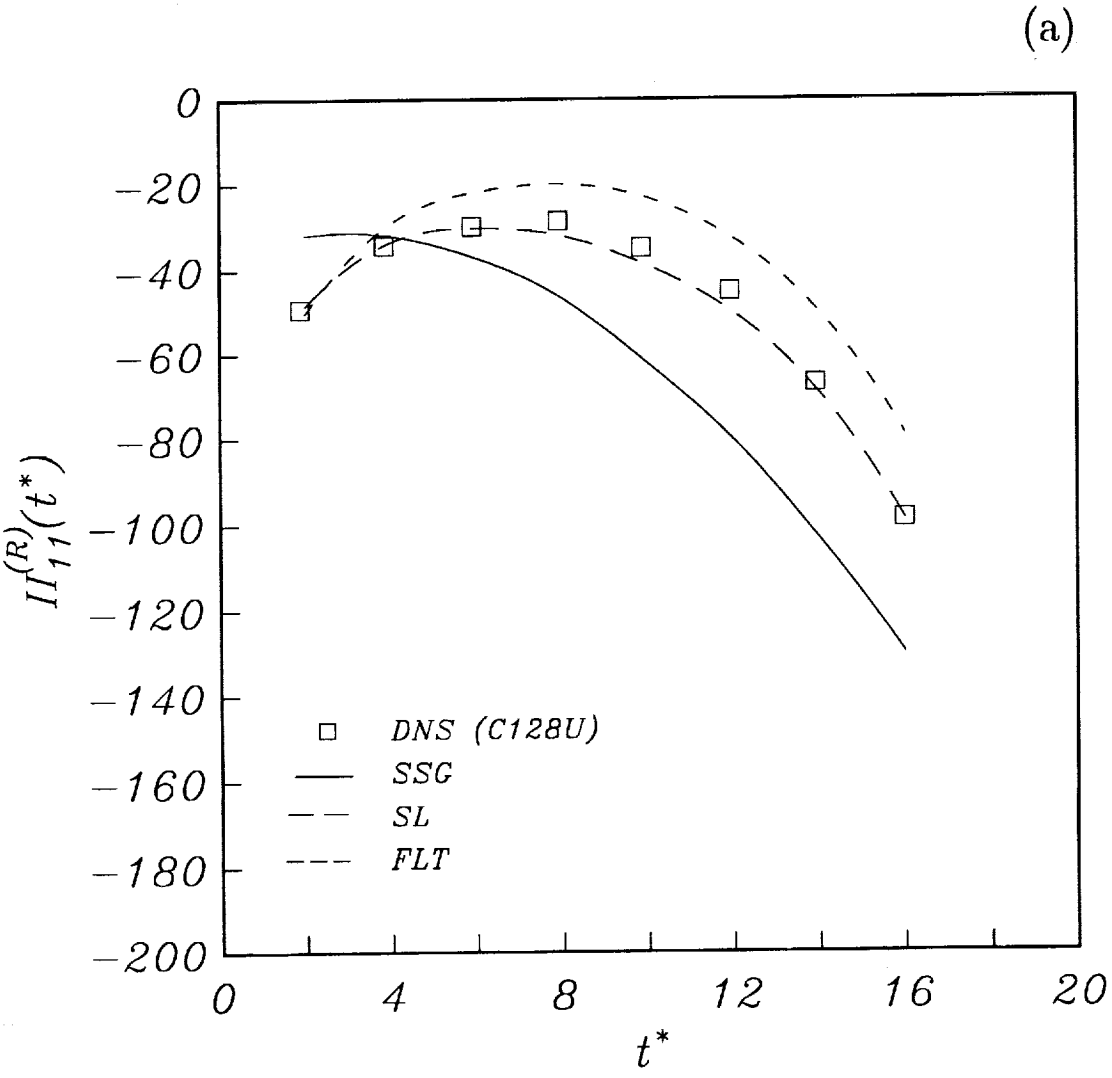

Figure 2. Comparison of the predictions of the SL, FLT and SSG models for the "rapid" pressure-strain correlation with the DNS results of Rogers et al.[9] for homogeneous shear flow (run C128U). (a) $\Pi_{11}^{(R)}$ component, (b) $\Pi_{12}^{(R)}$ component, and (c) $\Pi_{22}^{(R)}$ component.

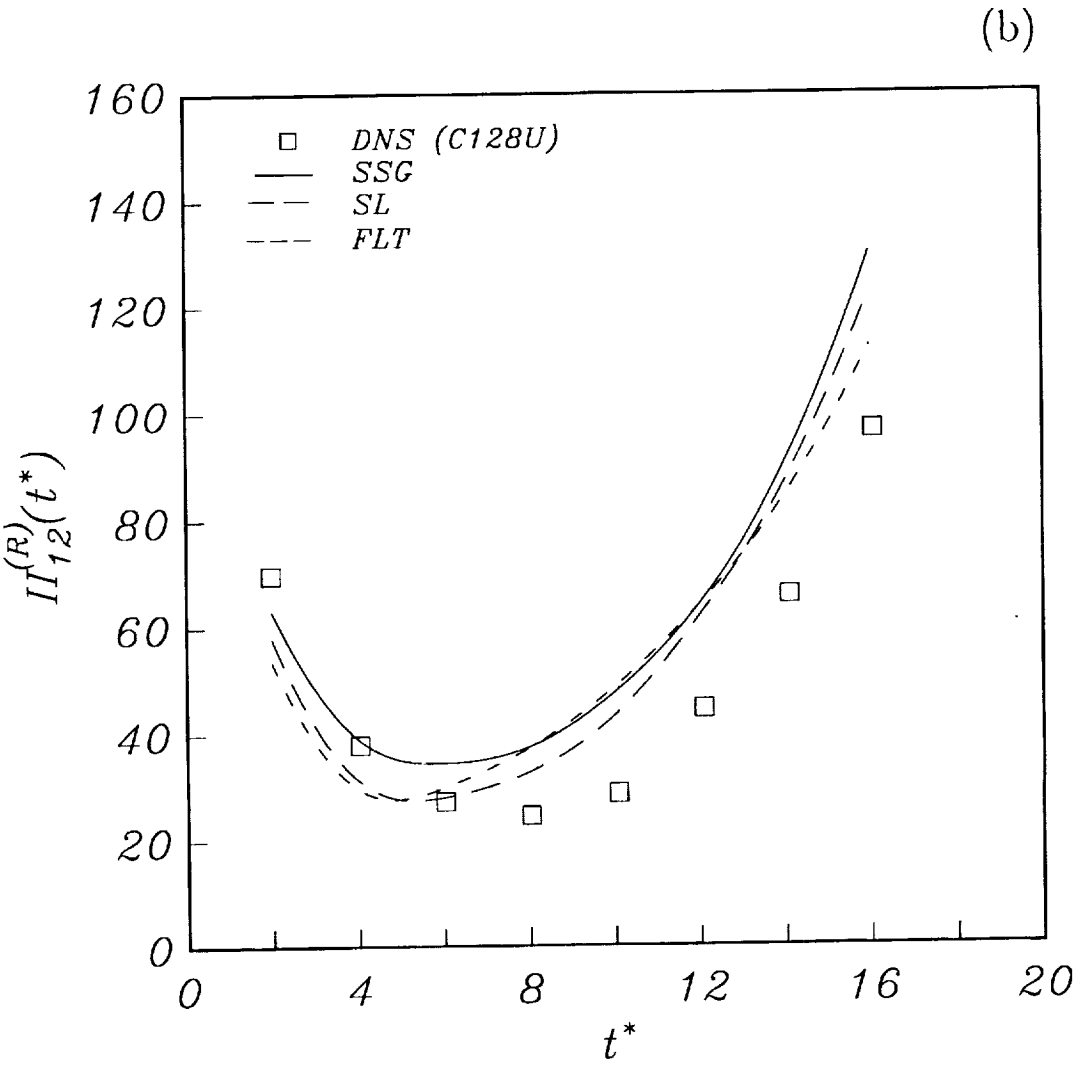

Figure 2. Comparison of the predictions of the SL, FLT and SSG models for the "rapid" pressure-strain correlation with the DNS results of Rogers et al.[9] for homogeneous shear flow (run C128U). (a) $\Pi_{11}^{(R)}$ component, (b) $\Pi_{12}^{(R)}$ component, and (c) $\Pi_{22}^{(R)}$ component.

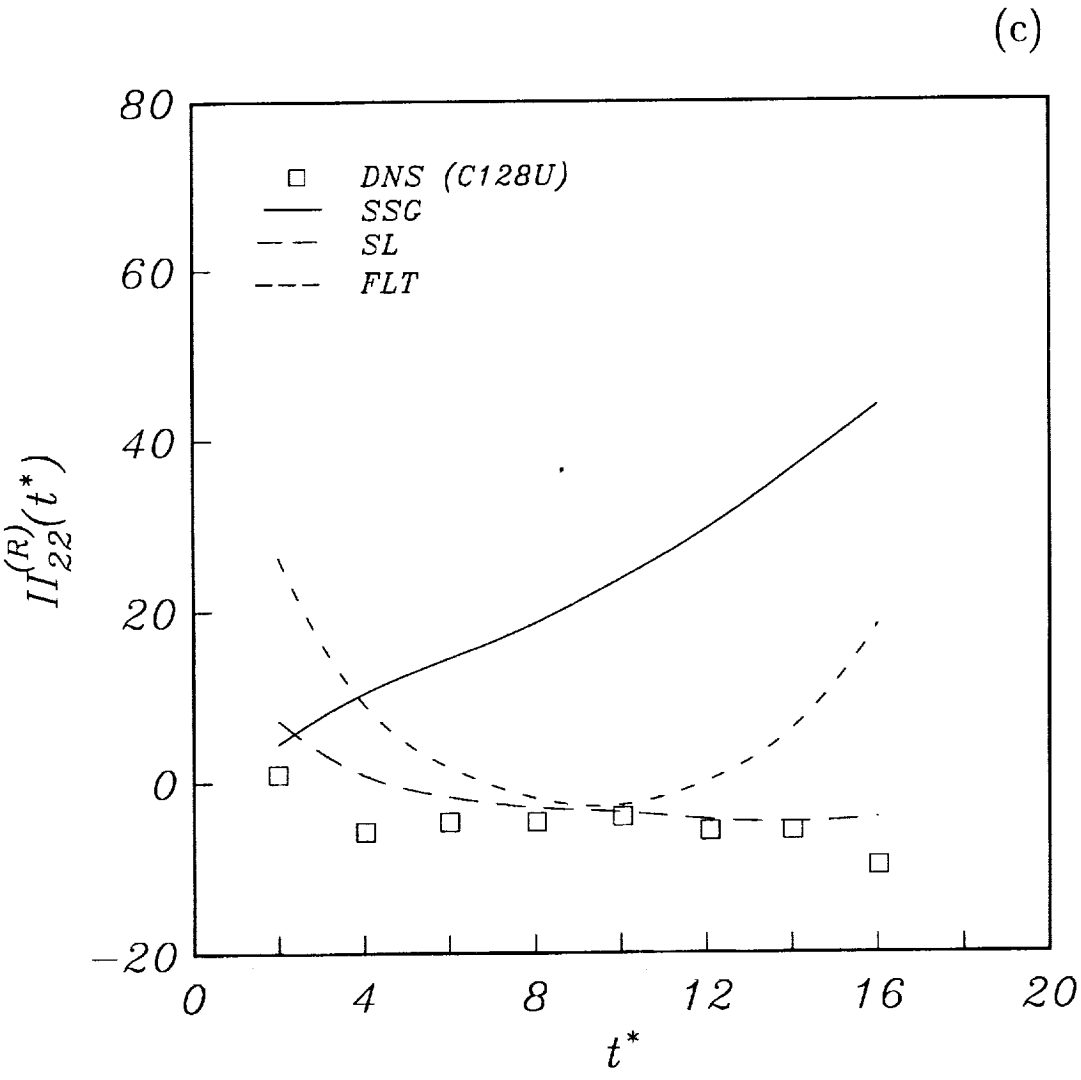

Figure 2. Comparison of the predictions of the SL, FLT and SSG models for the "rapid" pressure-strain correlation with the DNS results of Rogers et al.[9] for homogeneous shear flow (run C128U). (a) $\Pi_{11}^{(R)}$ component, (b) $\Pi_{12}^{(R)}$ component, and (c) $\Pi_{22}^{(R)}$ component.

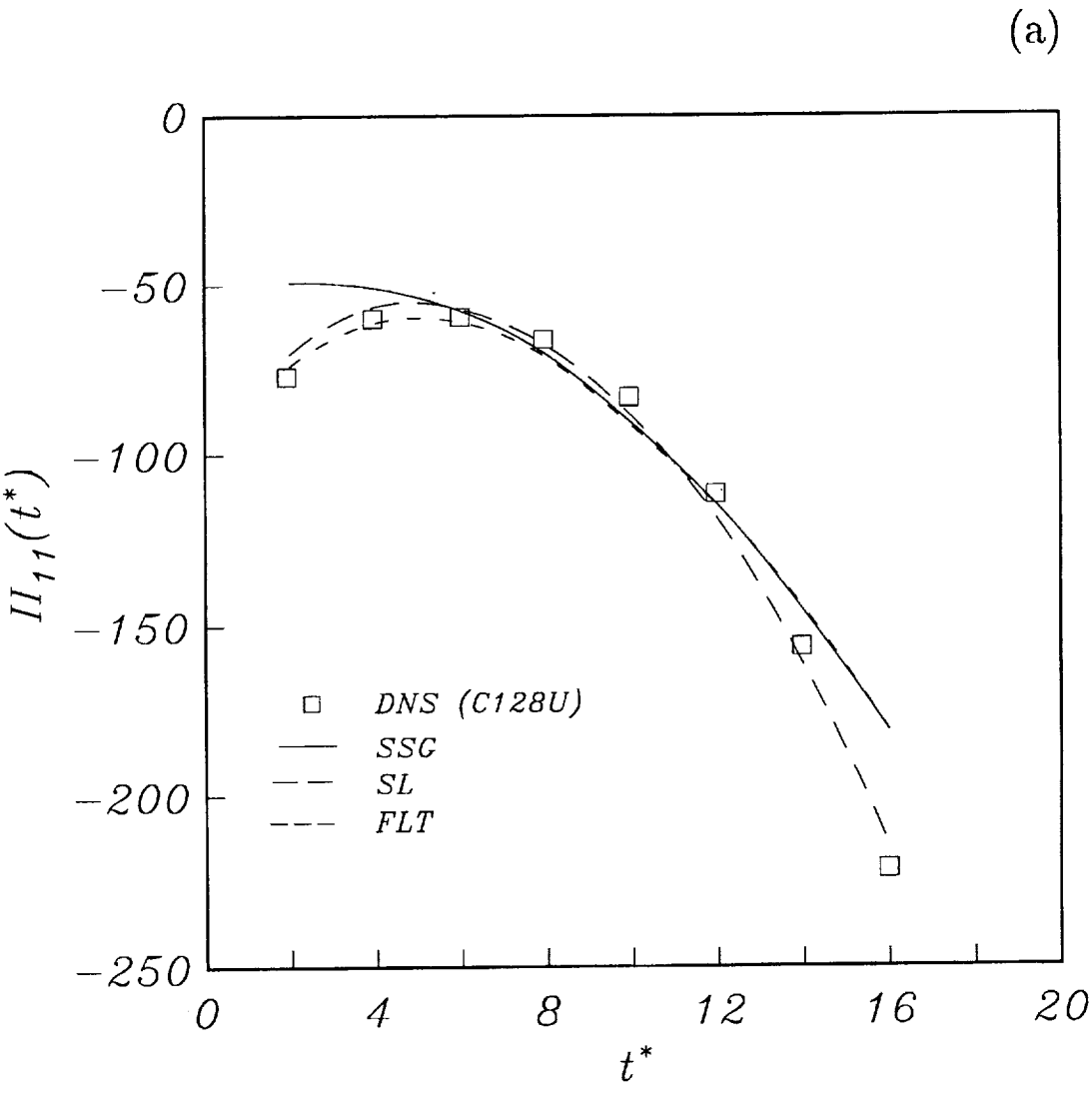

Figure 3. Comparison of the predictions of the SL, FLT and SSG models for the total pressure-strain correlation with the DNS results of Rogers et al.[9] for homogeneous shear flow (run C128U). (a) Π_{11} component, (b) Π_{12} component, and (c) Π_{22} component.

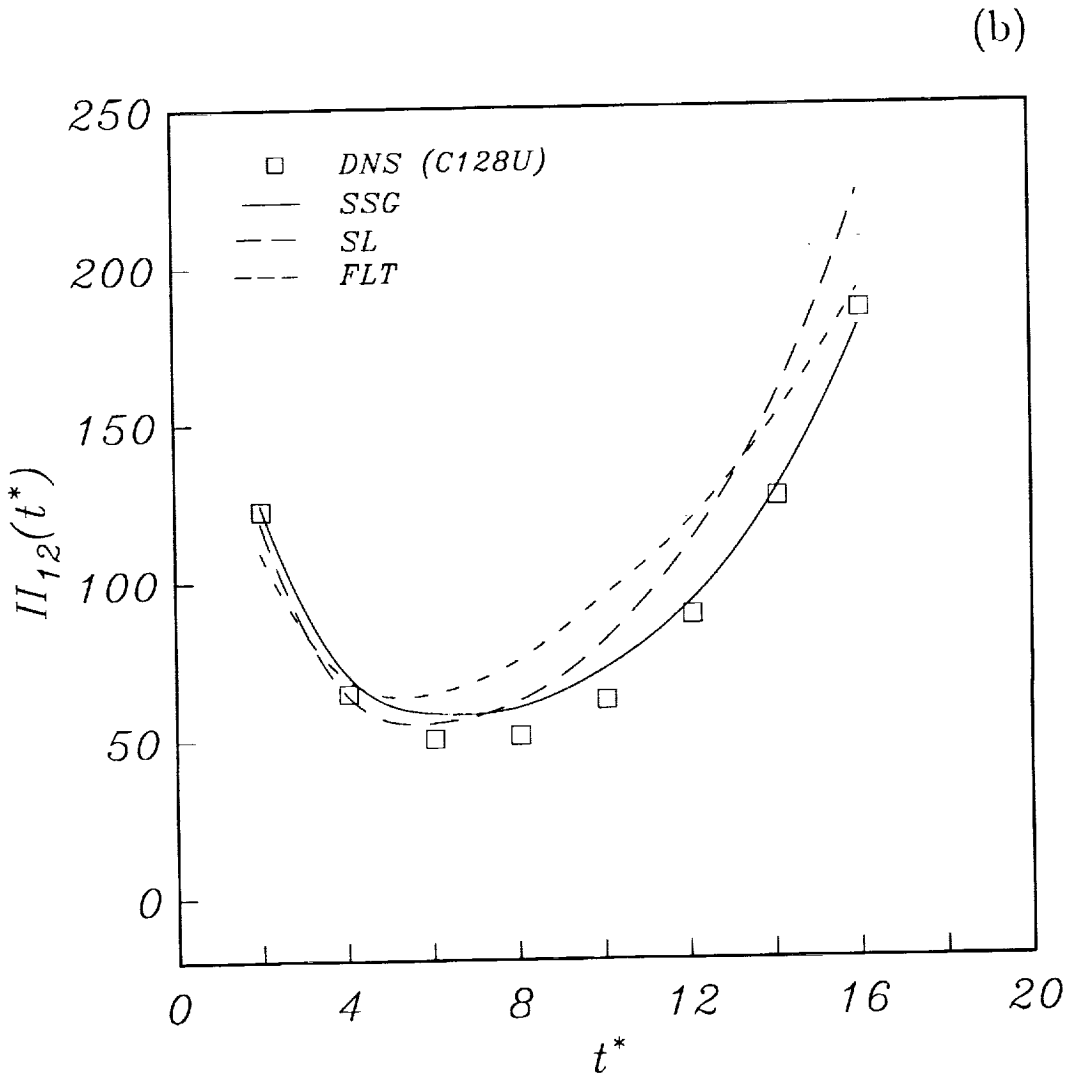

Figure 3. Comparison of the predictions of the SL, FLT and SSG models for the total pressure-strain correlation with the DNS results of Rogers et al.[9] for homogeneous shear flow (run C128U). (a) Π_{11} component, (b) Π_{12} component, and (c) Π_{22} component.

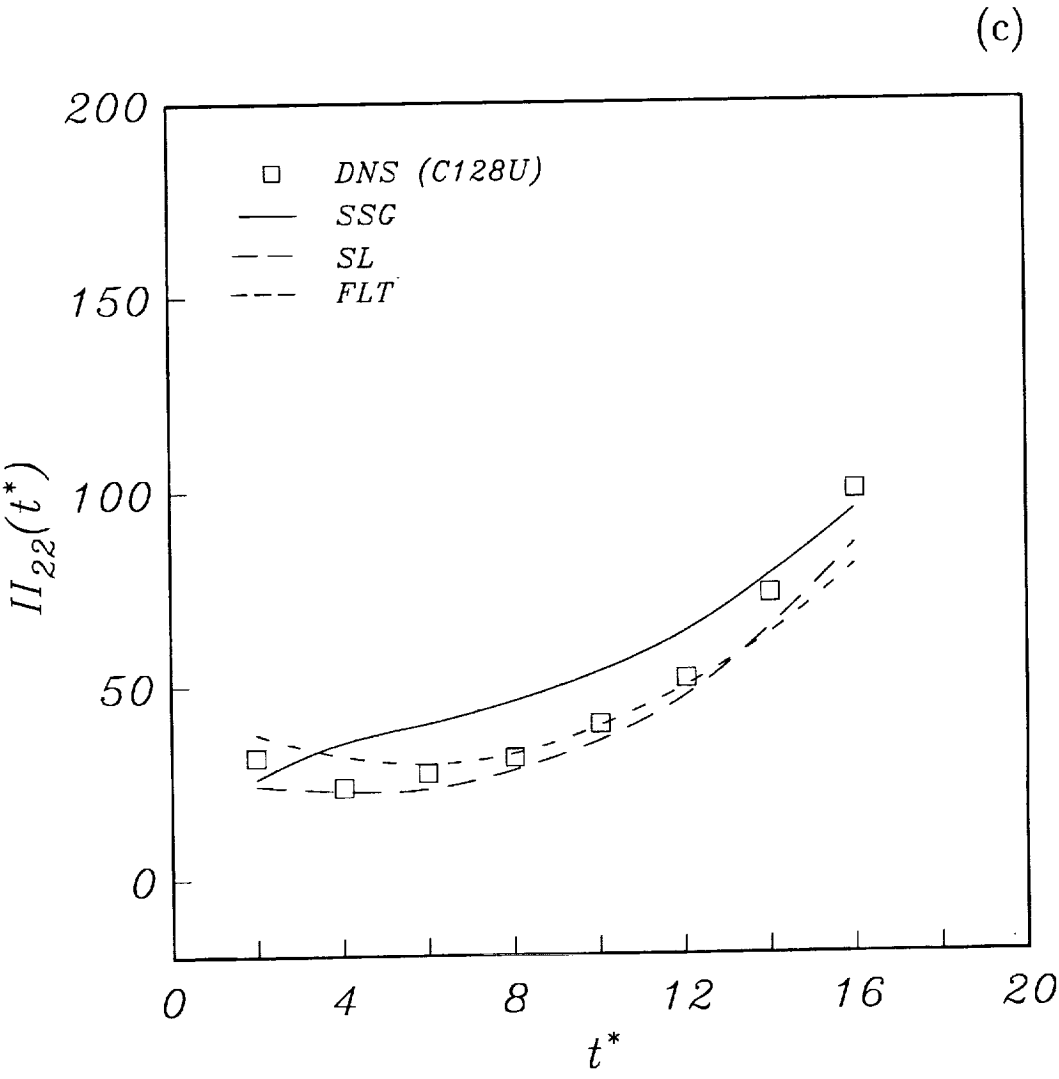

Figure 3. Comparison of the predictions of the SL, FLT and SSG models for the total pressure-strain correlation with the DNS results of Rogers et al.[9] for homogeneous shear flow (run C128U). (a) Π_{11} component, (b) Π_{12} component, and (c) Π_{22} component.

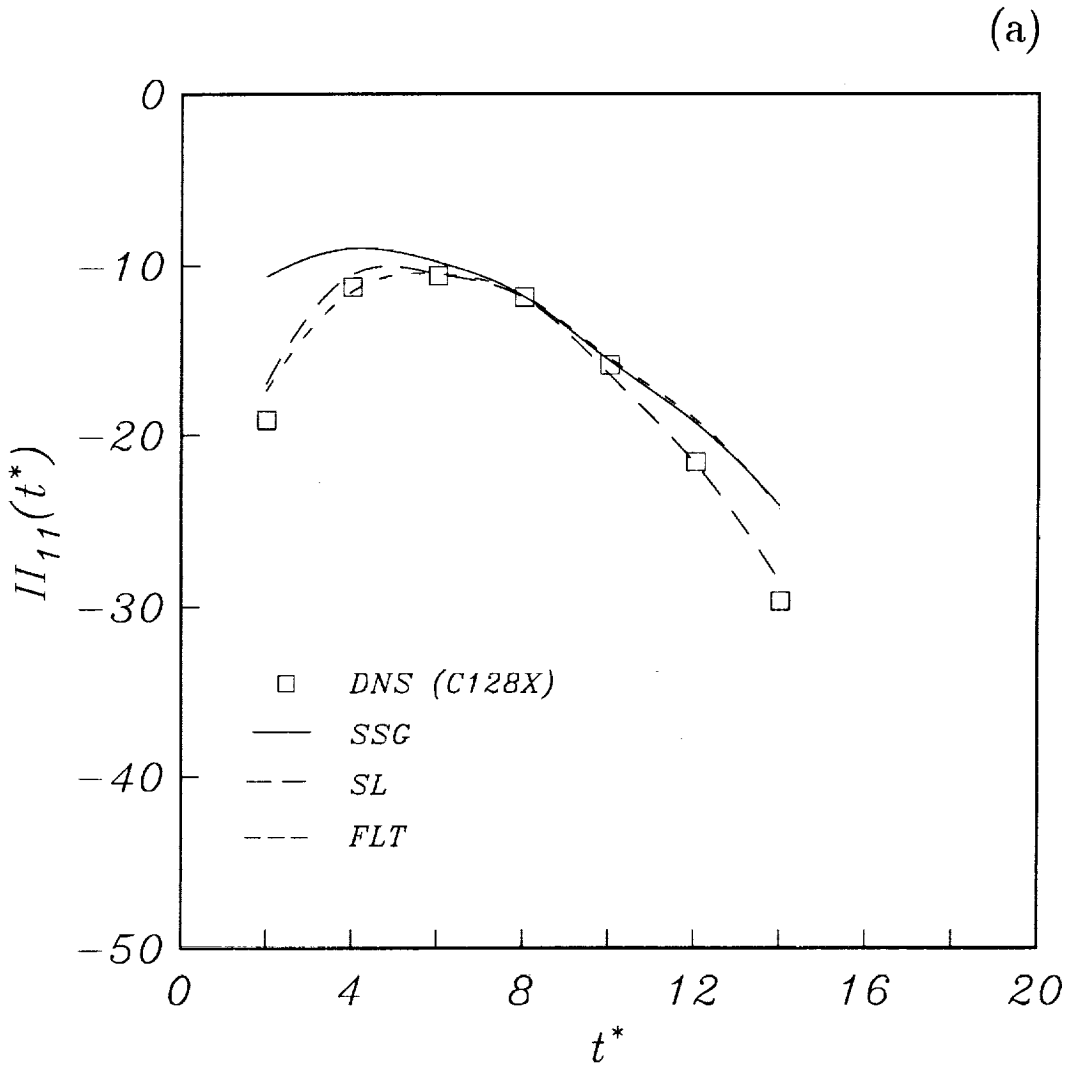

Figure 4. Comparison of model predictions for run C128X of Rogers et al.[9] (other details are the same as in Figure 3).

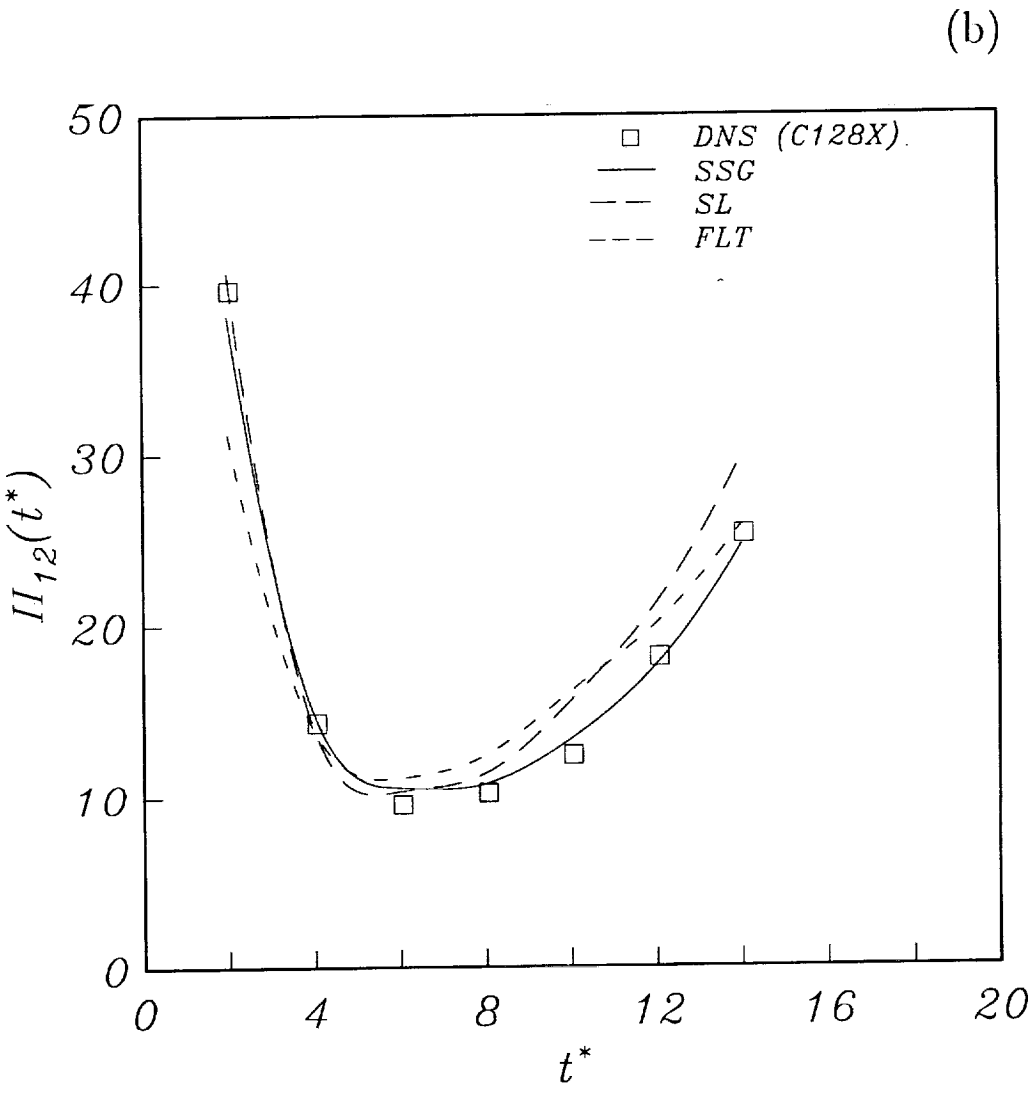

Figure 4. Comparison of model predictions for run C128X of Rogers et al.[9] (other details are the same as in Figure 3).

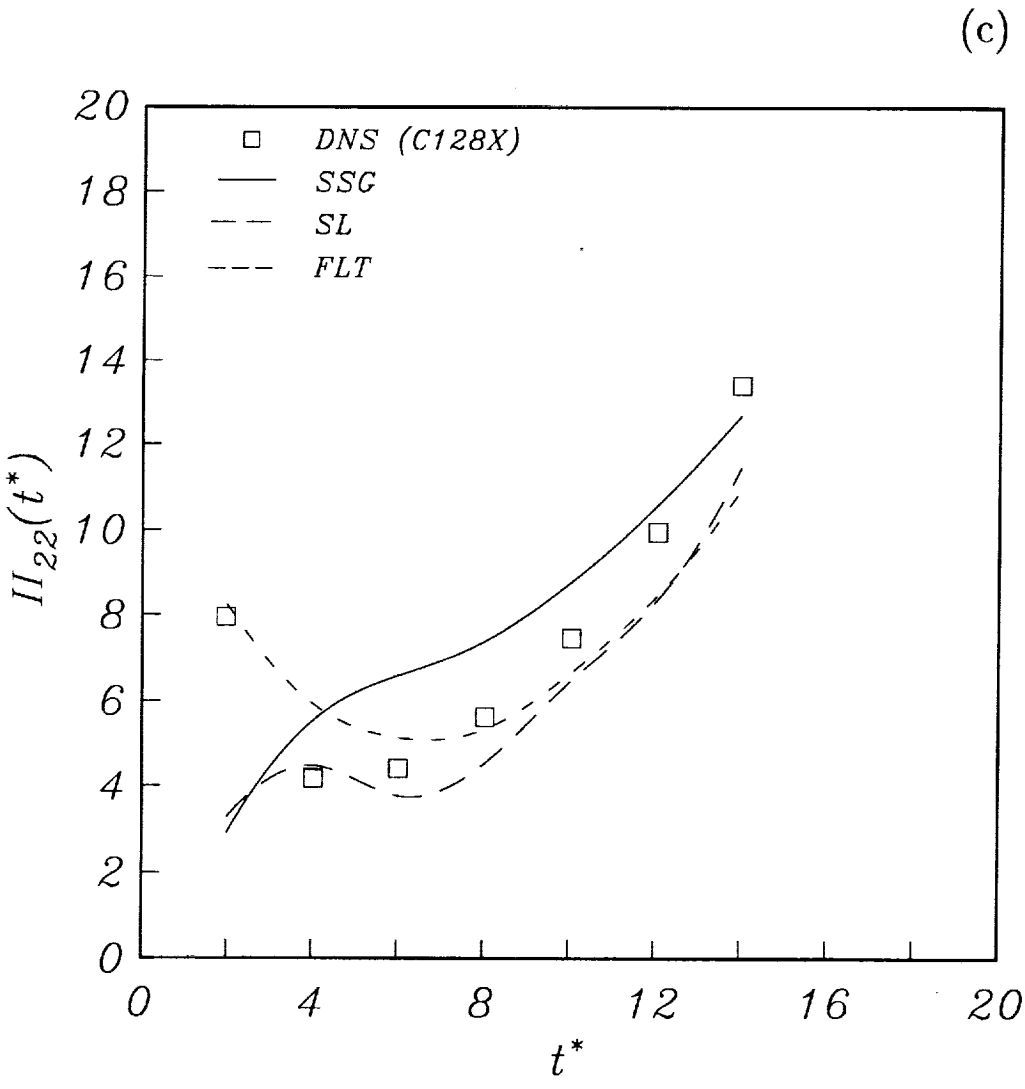

Figure 4. Comparison of model predictions for run C128X of Rogers et al.[9] (other details are the same as in Figure 3).

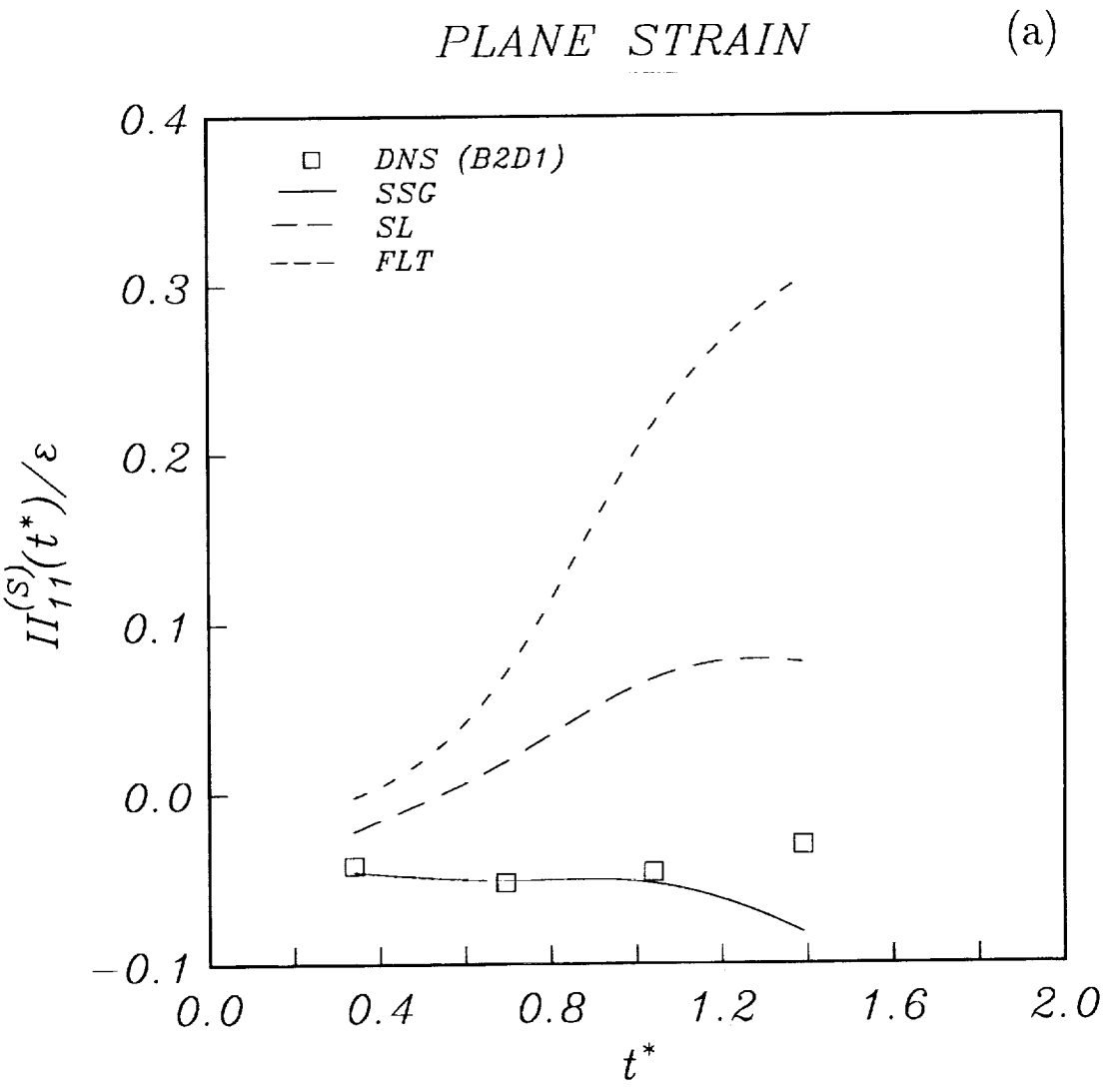

Figure 5. Time evolution of the dimensionless "slow" pressure-strain correlation in plane strain: Comparison of the model predictions with the DNS results of Rogallo[2] (run B2D1). (a) $\Pi_{11}^{(S)}$ component, (b) $\Pi_{22}^{(S)}$ component and (c) $\Pi_{33}^{(S)}$ component.

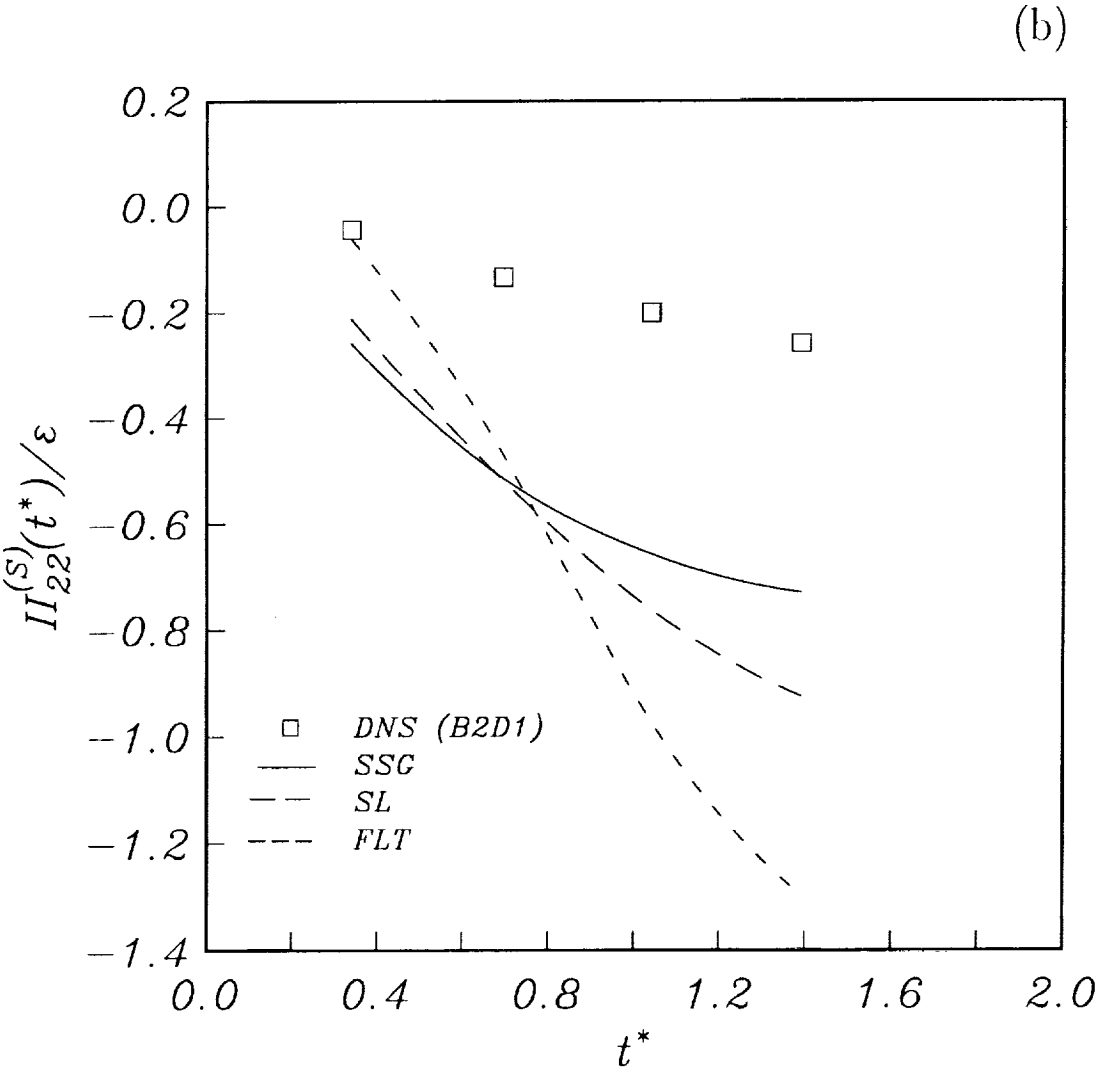

Figure 5. Time evolution of the dimensionless "slow" pressure-strain correlation in plane strain: Comparison of the model predictions with the DNS results of Rogallo[2] (run B2D1). (a) $\Pi_{11}^{(S)}$ component, (b) $\Pi_{22}^{(S)}$ component and (c) $\Pi_{33}^{(S)}$ component.

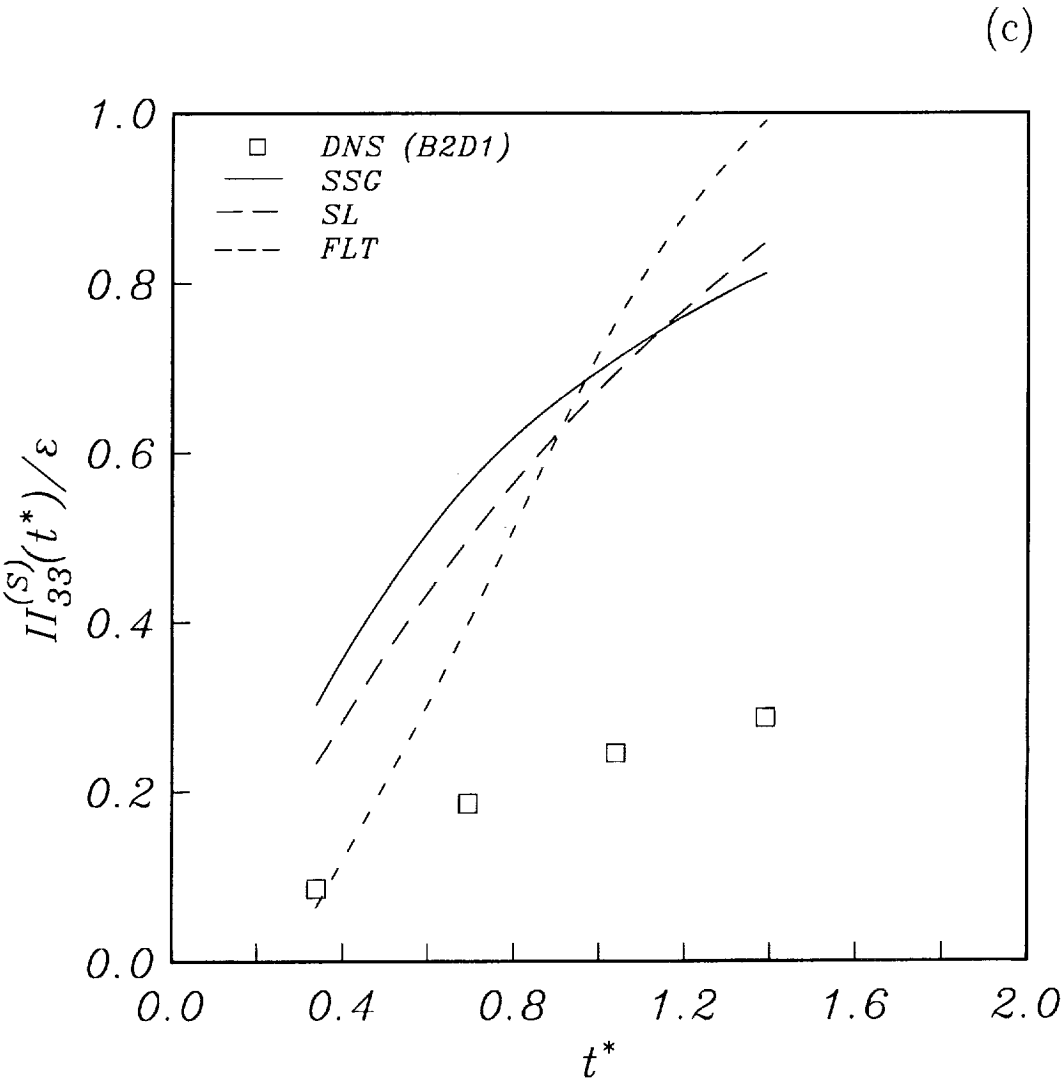

Figure 5. Time evolution of the dimensionless "slow" pressure-strain correlation in plane strain: Comparison of the model predictions with the DNS results of Rogallo[2] (run B2D1). (a) $\Pi_{11}^{(S)}$ component, (b) $\Pi_{22}^{(S)}$ component and (c) $\Pi_{33}^{(S)}$ component.

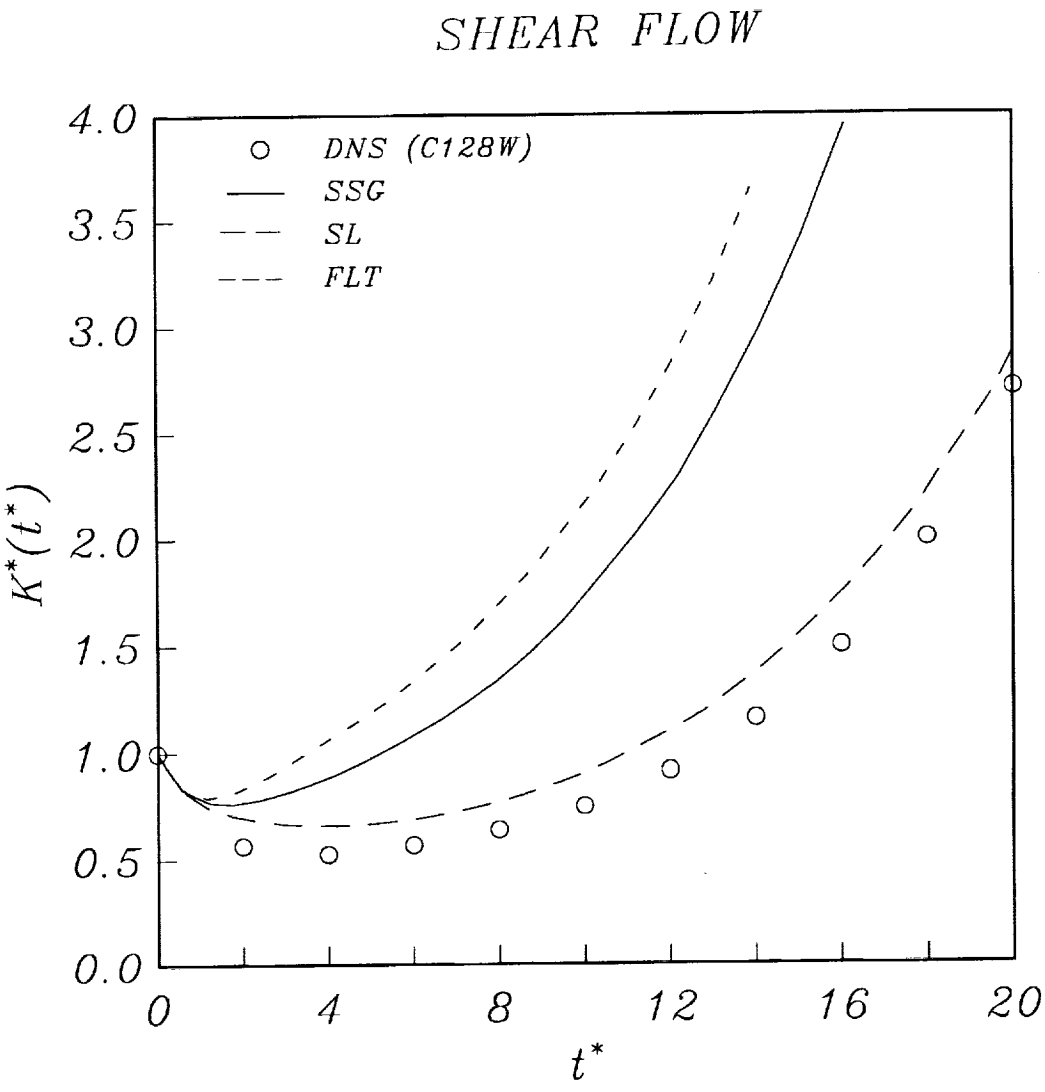

Figure 6. Time evolution of the turbulent kinetic energy in homogeneous shear flow: Comparison of the model calculations, starting from $St = 0$, with the DNS results of Rogers et al.[9] for run C128W.

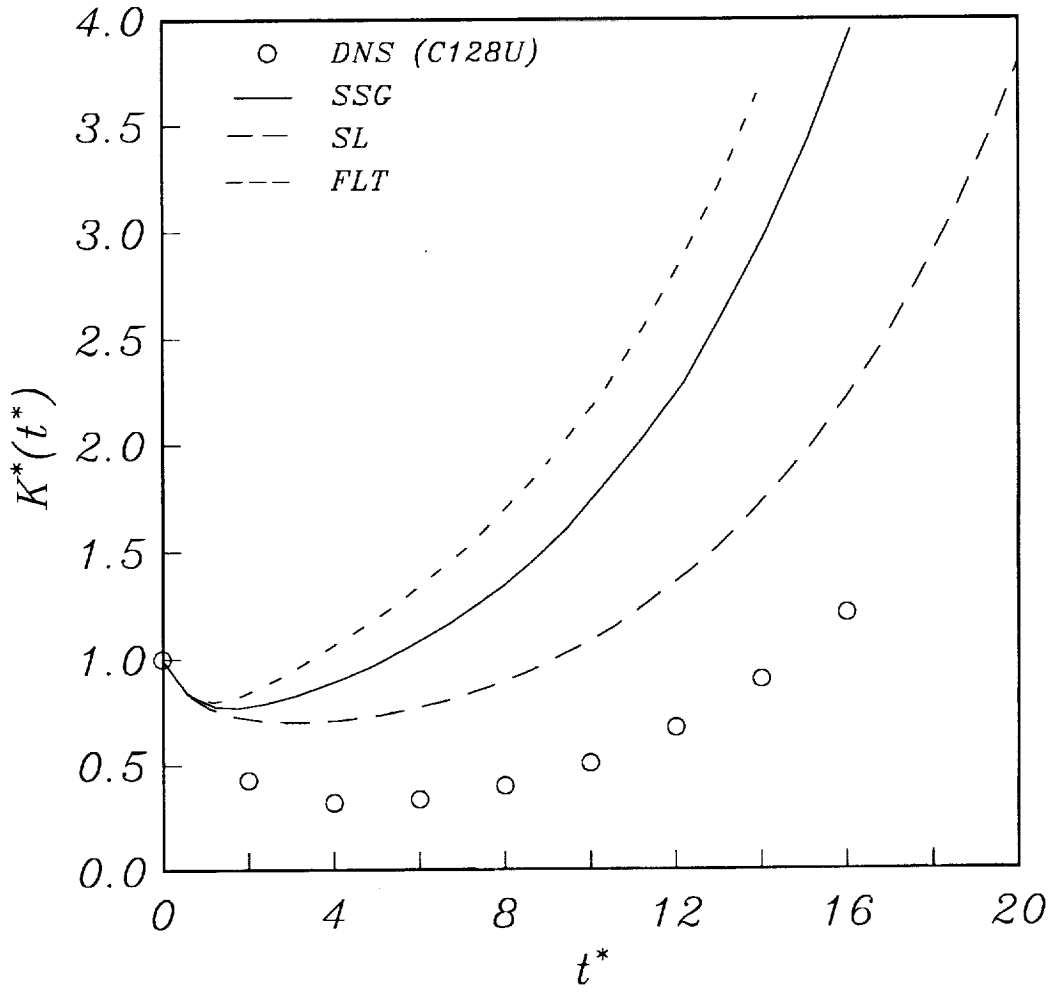

Figure 7. Comparison of models for run C128U (other details are the same as in Figure 6).

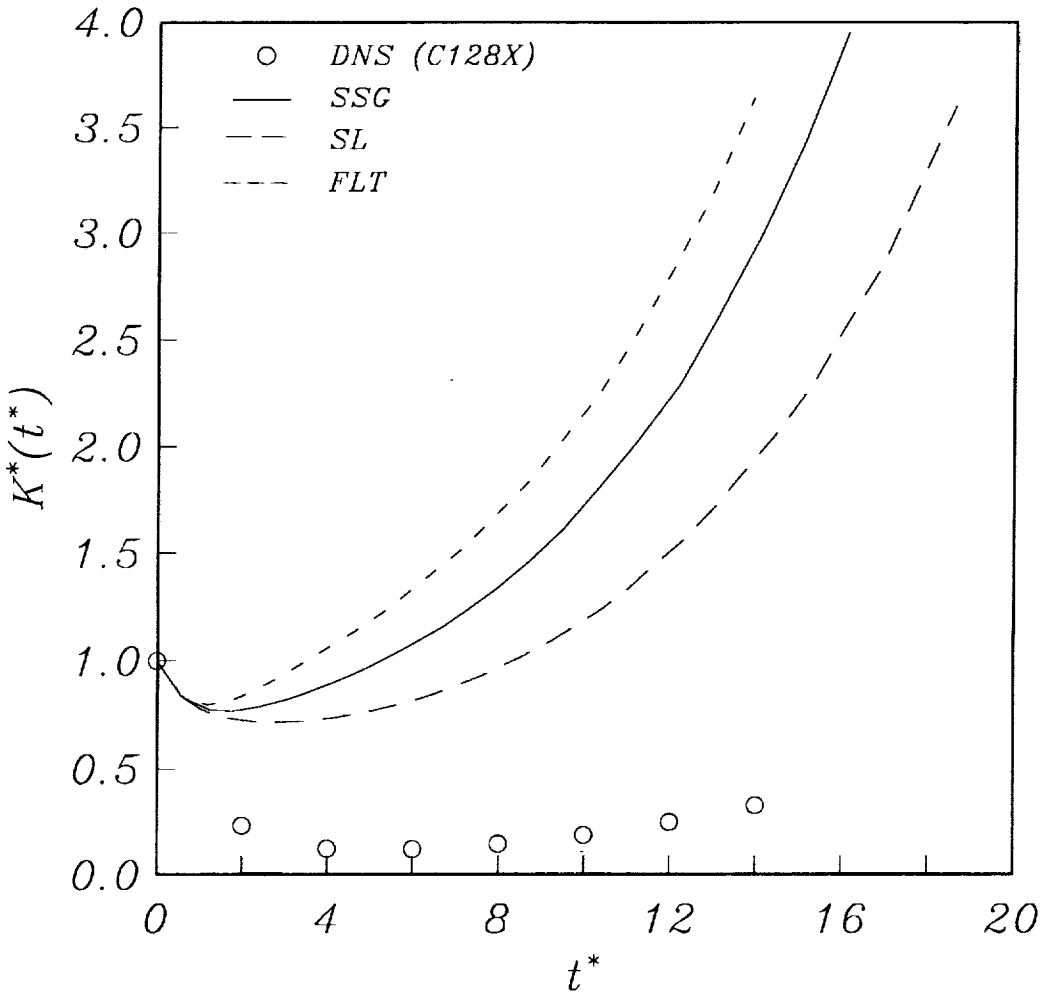

Figure 8. Comparison of models for run C128X (other details are same as in Figure 6).

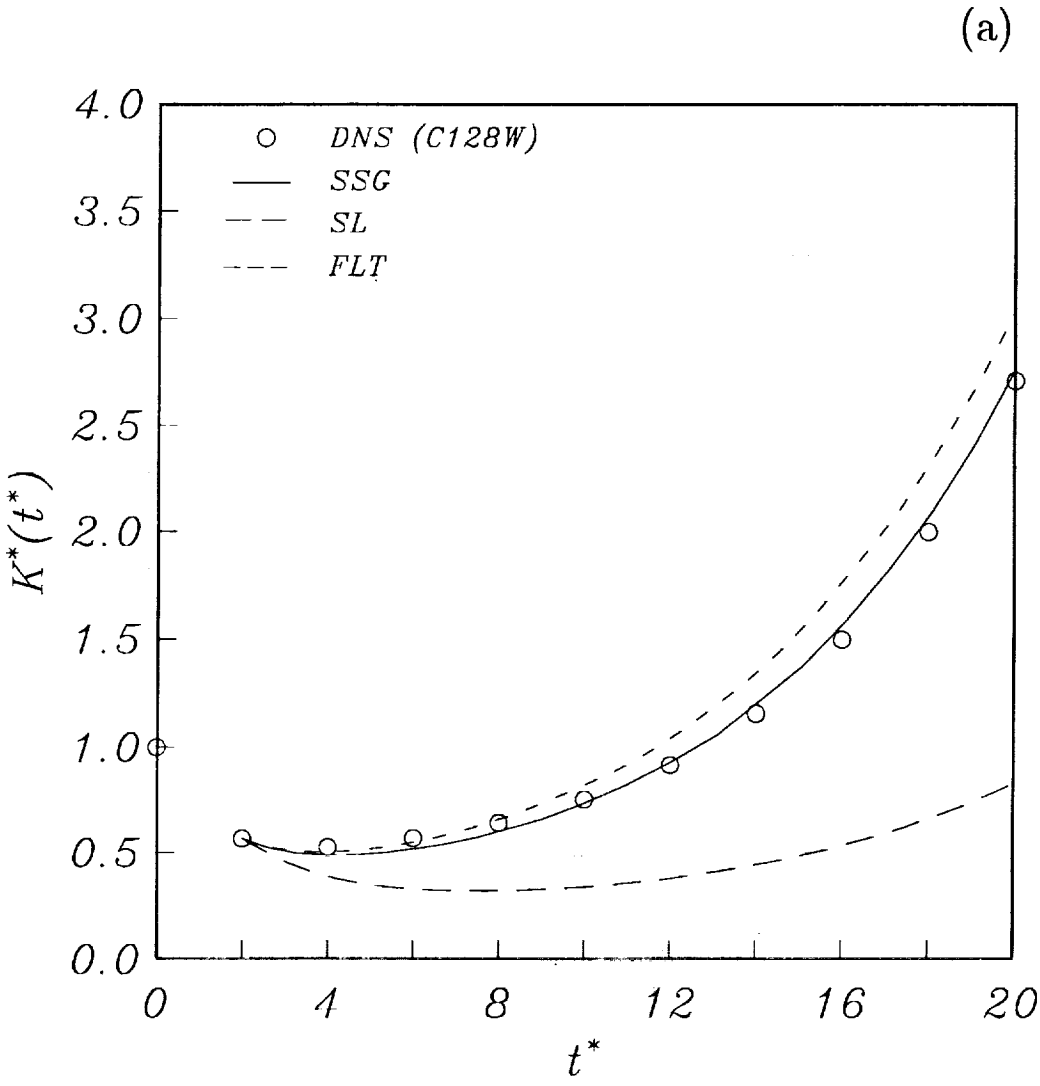

Figure 9. Time evolution of the turbulent kinetic energy in homogeneous shear flow: Comparison of the model calculations, starting from $St = 2$, with the DNS results of Rogers et al.[9] (a) Run C128W, (b) Run C128U and (c) Run C128X.

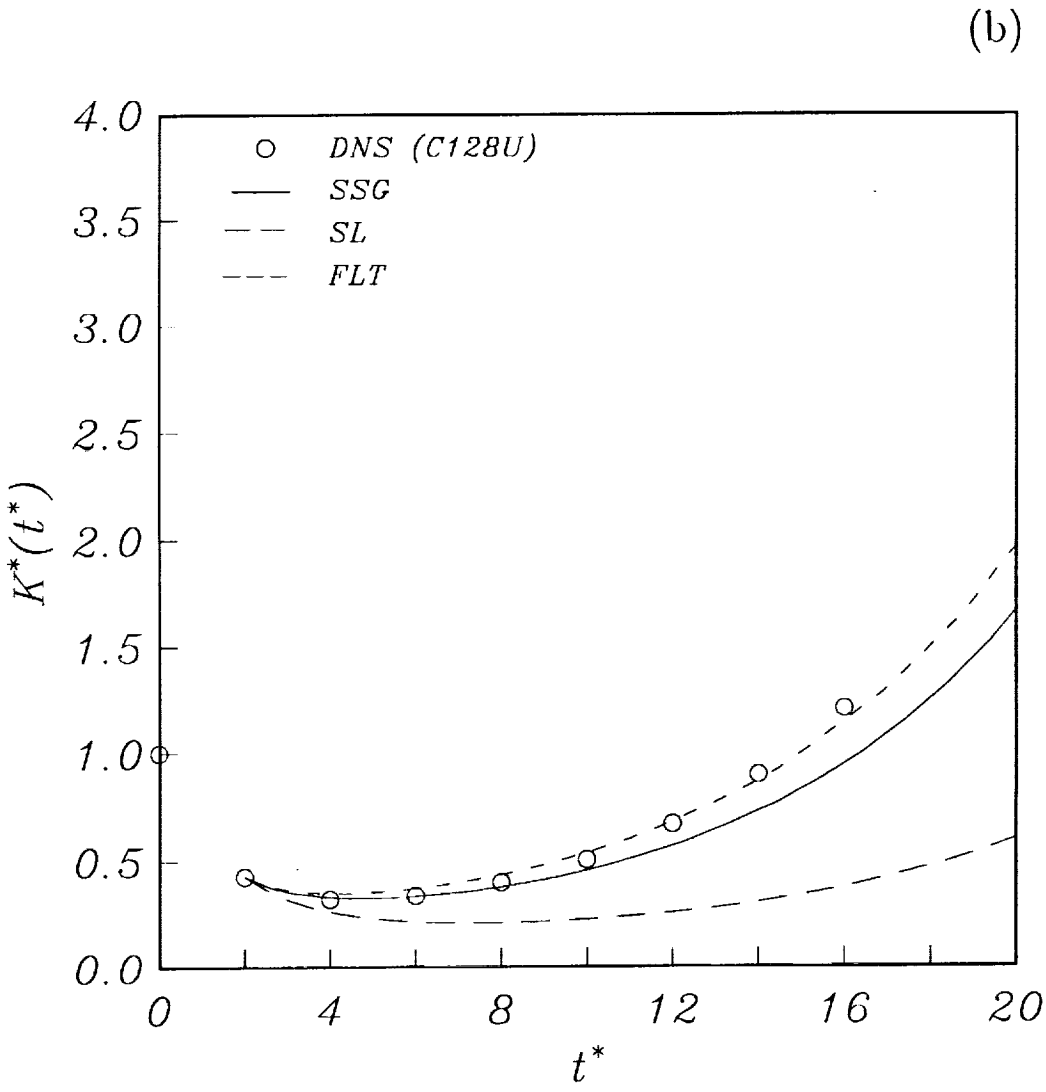

Figure 9. Time evolution of the turbulent kinetic energy in homogeneous shear flow: Comparison of the model calculations, starting from $St = 2$, with the DNS results of Rogers et al.[9] (a) Run C128W, (b) Run C128U and (c) Run C128X.

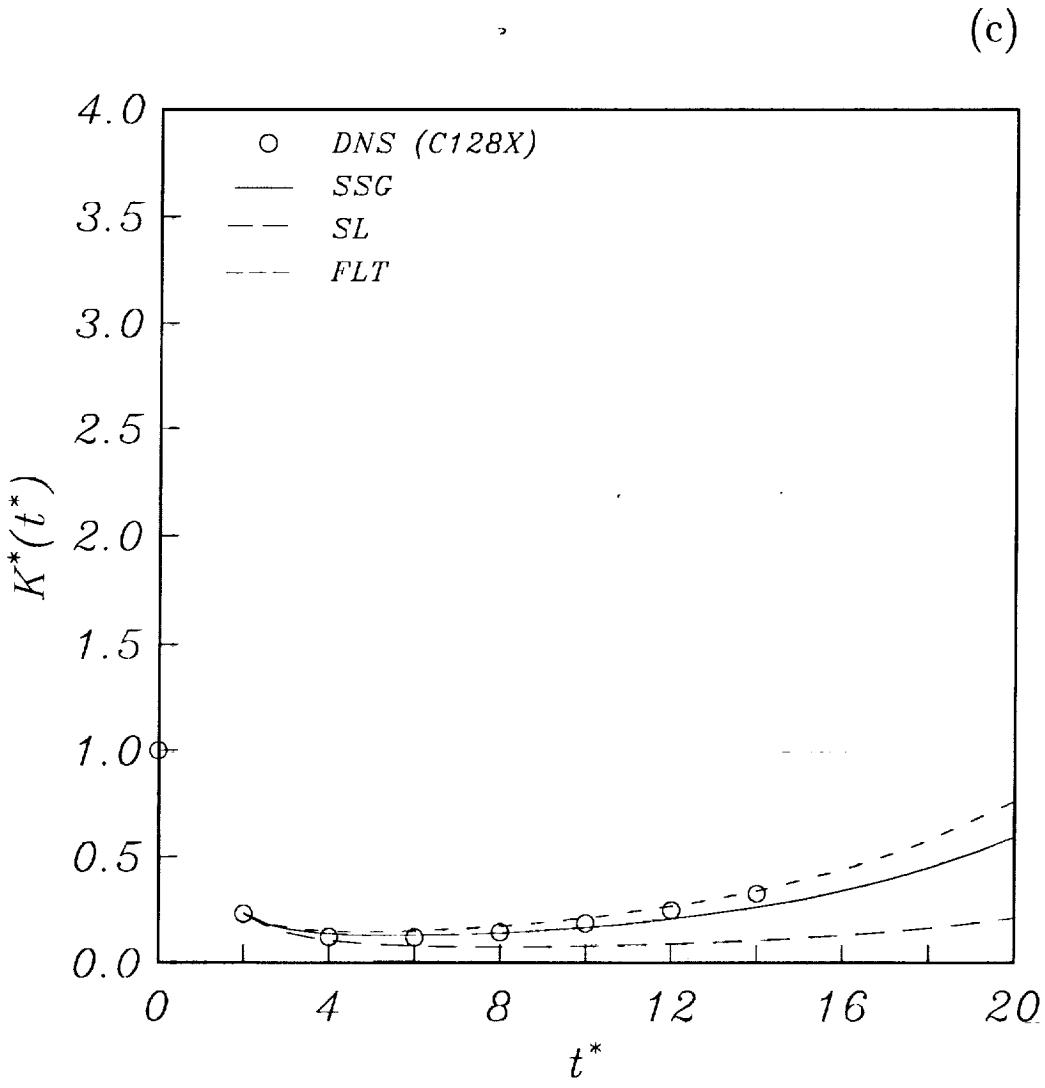

Figure 9. Time evolution of the turbulent kinetic energy in homogeneous shear flow: Comparison of the model calculations, starting from $St = 2$, with the DNS results of Rogers et al.[9] (a) Run C128W, (b) Run C128U and (c) Run C128X.

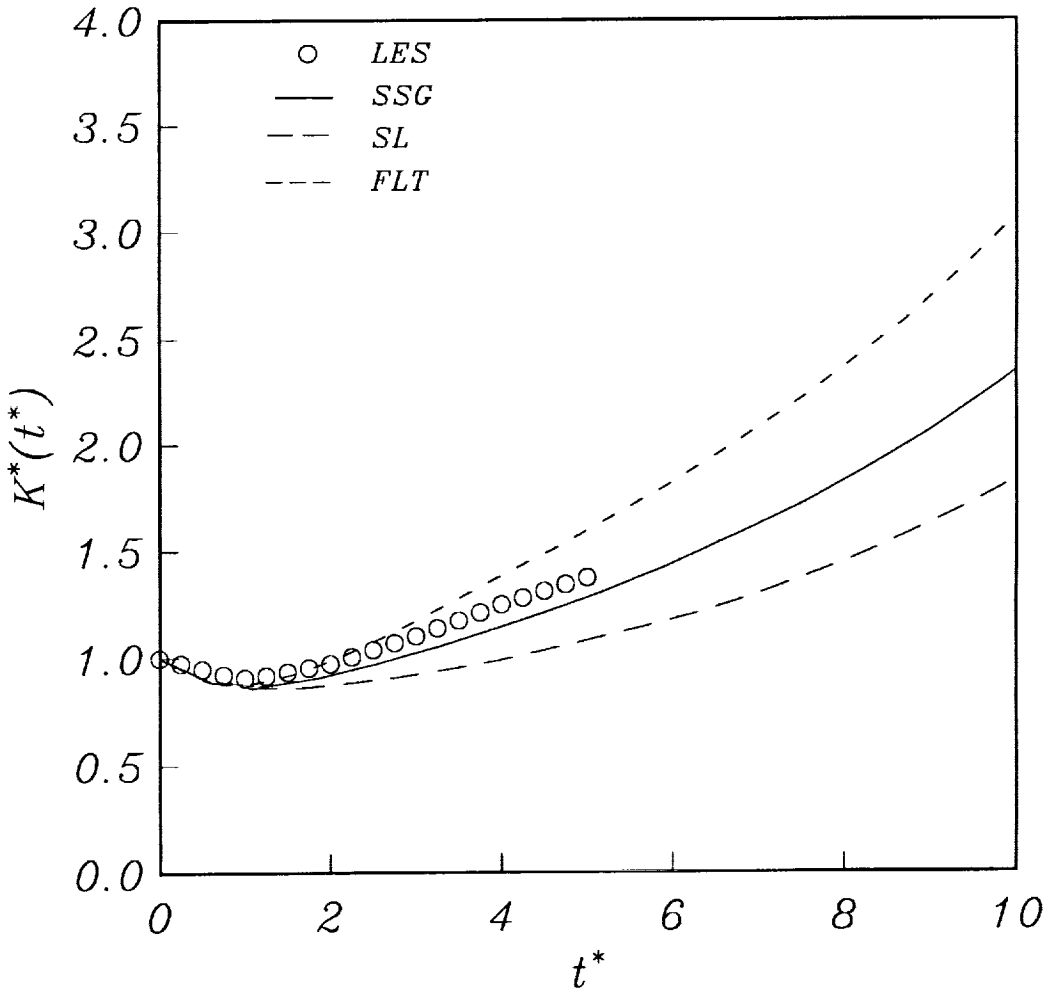

Figure 10. Comparison of the model predictions for the time evolution of the turbulent kinetic energy with the large-eddy simulation (LES) of Bardina et al.[22] for homogeneous shear flow.

REPORT DOCUMENTATION PAGE

Form Approved
OMB No. 0704-0188

1. AGENCY USE ONLY (Leave blank)	2. REPORT DATE	3. REPORT TYPE AND DATES COVERED
	April 1992	Contractor Report

4. TITLE AND SUBTITLE

ON TESTING MODELS FOR THE PRESSURE-STRAIN CORRELATION OF TURBULENCE USING DIRECT SIMULATIONS

5. FUNDING NUMBERS

C NAS1-18605

WU 505-90-52-01

6. AUTHOR(S)

C. G. Speziale
T. B. Gatski
S. Sarkar

7. PERFORMING ORGANIZATION NAME(S) AND ADDRESS(ES)

Institute for Computer Applications in Science and Engineering
Mail Stop 132C, NASA Langley Research Center
Hampton, VA 23665-5225

8. PERFORMING ORGANIZATION REPORT NUMBER

ICASE Report No. 92-16

9. SPONSORING/MONITORING AGENCY NAME(S) AND ADDRESS(ES)

National Aeronautics and Space Administration
Langley Research Center
Hampton, VA 23665-5225

10. SPONSORING/MONITORING AGENCY REPORT NUMBER

NASA CR-189638
ICASE Report No. 92-16

11. SUPPLEMENTARY NOTES

Langley Technical Monitor: Michael F. Card
Final Report

To be submitted to Physics of Fluids A

12a. DISTRIBUTION/AVAILABILITY STATEMENT

Unclassified - Unlimited
Subject Category 34

12b. DISTRIBUTION CODE

13. ABSTRACT *(Maximum 200 words)*

Direct simulations of homogeneous turbulence have, in recent years, come into widespread use for the evaluation of models for the pressure-strain correlation of turbulence. While work in this area has been beneficial, the increasingly common practice of testing the slow and rapid parts of these models separately in uniformly strained turbulent flows is shown in this paper to be unsound. For such flows, the decomposition of models for the pressure-strain correlation into slow and rapid parts is ambiguous. Consequently, when tested in this manner, misleading conclusions can be drawn about the performance of pressure-strain models. This point is amplified by illustrative calculations of homogeneous shear flow where other pitfalls in the evaluation of models are also uncovered. More meaningful measures for testing the performance of pressure-strain models in uniformly strained turbulent flows are proposed and the implications for turbulence modeling are discussed.

14. SUBJECT TERMS	15. NUMBER OF PAGES
pressure-strain correlation; direct simulations; second-order closure models	42
	16. PRICE CODE A03

17. SECURITY CLASSIFICATION OF REPORT	18. SECURITY CLASSIFICATION OF THIS PAGE	19. SECURITY CLASSIFICATION OF ABSTRACT	20. LIMITATION OF ABSTRACT
Unclassified	Unclassified		